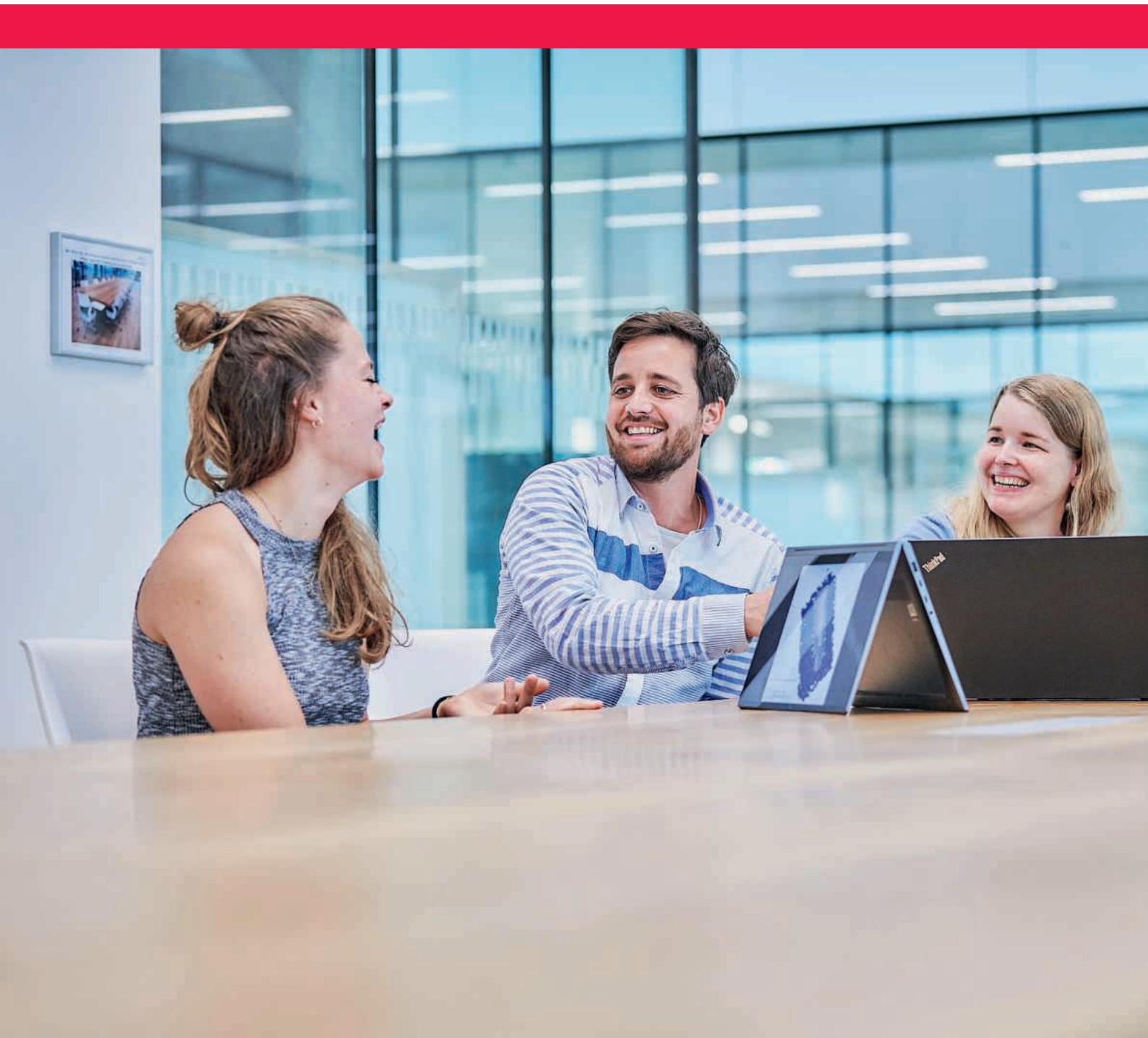


Master Biomedical Engineering

# Annual Report 2020



# MASTER OF SCIENCE IN BIOMEDICAL ENGINEERING

## Contents

Introduction.....	3
Organization.....	3
Structure of Courses in the Master's Program.....	4
Major Modules .....	6
Evaluation of Courses in the Year 2020.....	9
RMS Award .....	9
Faculty.....	10
Statistics .....	11
Graduate Profile.....	12
The Biomedical Engineering Club.....	13
Master's Theses 2020.....	14

## Imprint

Master's Program Biomedical Engineering Annual Report 2020

### Editor

University of Bern  
Master's Program Biomedical Engineering

### Layout/Print

Länggass Druck AG Bern  
Länggassstrasse 65  
3001 Bern

### Photo front page

Adrian Moser, Bern

### Photo back page

Volker M. Koch

## Introduction

After integration of the Institute of Surgical Technology and Biomechanics (ISTB) in the ARTORG Center for Biomedical Engineering Research and the move of the study coordination to the Swiss Institute for Translational and Entrepreneurial Medicine (SITEM) in 2019, we were looking for a quiet, transition year to adjust to these rather major changes...

Needless to say that we did not expect a pandemic crisis with a transition from presence to online learning within three days in March and fully online examinations in June. Fortunately, the University of Bern provided rapidly an efficient IT platform, the necessary software and a diligent support to manage the technical aspects of this transition.

At this place, I wish to address hereby my deepest appreciation to the teachers and the members of the study coordination for overcoming what is probably the highest challenge that had to be faced since the birth of the BME program. The students should also be acknowledged for their understanding and perseverance in this confined learning.

The euphoria of overcoming the partial lockdown with online tools in the spring was progressively replaced by the awareness of the various limitations of this pedagogical scenario in the fall. Practical courses could not take place, master theses had to be reprogrammed and everyone agree that the lack of interactions degraded the quality of the learning process.

Nevertheless, we have to admit that this drop in the cold water accelerated our confrontation with online education. We learned about innovative technical solutions, shared experience among teachers, improved our ability to select the appropriate tools for specific tasks and found new ways to design examinations. However, we also learned that online written examinations are everything but satisfactory and should probably be avoided in the future.

Sadly, the Biomedical Engineering Day had to be cancelled and no live surgery could be retransmitted. However, we decided to maintain our awards despite the lack of audience. On the one hand, the RMS Award was attributed to Michal Hayoz for a remarkable overall grade average of 5.89/6.0. On the other hand, the Best Abstract Award of the BME club was given to Ms Giuditta Thoma for her master thesis entitled "Lung-Alveoli-on-Chip: Mechanical Characterization of a New Biological Membrane". Congratulations to both of them.

This year, the number of starting students reached 61, which represents a slight but encouraging increase with respect to previous years. The independent evaluation of the courses by the University of Bern indicates that despite the difficult conditions, the teachers managed to keep the interest, motivation and satisfaction of the students at a reasonable level.

In conclusion, this was an exhausting year for academic education, but we are relieved and grateful that most courses could be maintained, the examinations could take place and the students could continue their education. We are highly motivated to exploit the gained experience

for improving the program along several avenues that were identified in 2020. Thank you for your interest in our program and enjoy the reading.



Philippe Zysset  
Program Director

## Organization

### Management



Ph. Zysset  
Program Director, University of Bern



V. M. Koch  
Deputy Program Director,  
Bern University of Applied Sciences

### Administration



U. Jakob-Burger  
Study Coordinator, University of Bern



C. Karaca  
Study Coordinator, Bern University of Applied Sciences



A. Neuenschwander Salazar  
Study Coordinator, University of Bern



J. Spyra  
Event Organization, University of Bern



Ph. Büchler  
Master Thesis Coordinator, University of Bern

## Structure of Courses in the Master's Program

Since the start of the Master's Program Biomedical Engineering in March 2006, the constant effort to improve the quality of our curriculum has resulted in substantial changes of the course structure over the past years. The first curriculum consisted of a number of individual courses that were either mandatory or elective, but their coherence with regards to contents was in most cases not expressed by a defined structure. However, two major modules (formerly called "focus areas") already existed.

As of Fall Semester 2009, all courses were grouped in a strictly modular way in order to enhance both the clarity and the flexibility of the curricular structure. A main idea was to guide the students through their studies in a better way by adding an elective part to the major modules, which formerly had consisted exclusively of mandatory courses. Besides, the curriculum was expanded by a number of new specialized courses as well as an additional major module called "Image-Guided Therapy".

Adaptations in the legal framework of the master's program are now offering more flexibility in the design of courses and modules, thus providing the basis for a second fundamental restructuring of the curriculum as of Fall Semester 2013. In particular, a module called "Complementary Skills" was introduced. In addition, the list of mandatory courses in both basic and major modules was revised.

More recently, in Fall Semester 2017, a module "preparation courses" was created. The courses in this module are intended to fill gaps regarding prerequisites for basic and advanced courses in the master's program Biomedical Engineering. In 2018, the basic module "Biomedical Engineering" was re-structured and augmented by new courses in "Medical Informatics" and "Introduction to Biomechanics".

## The Curriculum

### Duration of Studies and Part-Time Professional Occupation

The full-time study program takes 4 semesters, which corresponds to 120 ECTS credits, one ECTS credit being defined as 25–30 hours of student workload. It can be extended to a maximum of 6 semesters. When a student decides to complete the studies in parallel to a part-time professional occupation, further extension is possible on request. To support regular part-time work, mandatory courses take place (with rare exceptions) on only 3 days per week.

### Preparation Courses

Owing to the interdisciplinary nature of the BME master's program, our students come from various fields of study. Especially students with a non-engineering background – for example in medicine – do not fulfill all prerequisites for the courses of the master's program.

Therefore, introductory courses in MATLAB, C++ programming, Electrical Engineering and Engineering Mechanics as well as the tutorial-based course "Selected Chapters in Mathematics" were introduced and allow to create a tailor-made curriculum for these students. Students with a background in engineering, on the other hand, have the possibility to select these courses freely if they feel the need to refresh some of the knowledge provided.

### Basic Modules

The basic modules provide the students with the necessary background to be able to fully understand the complex subject matter in the specialized courses. All students have to complete all courses in the Basic Modules Human Medicine, Applied Mathematics, and Biomedical Engineering. In the first semester, all mandatory courses belong to this group, whereas in the second and third semester, the courses from the basic modules make up for approximately 30 %.

### Major Modules

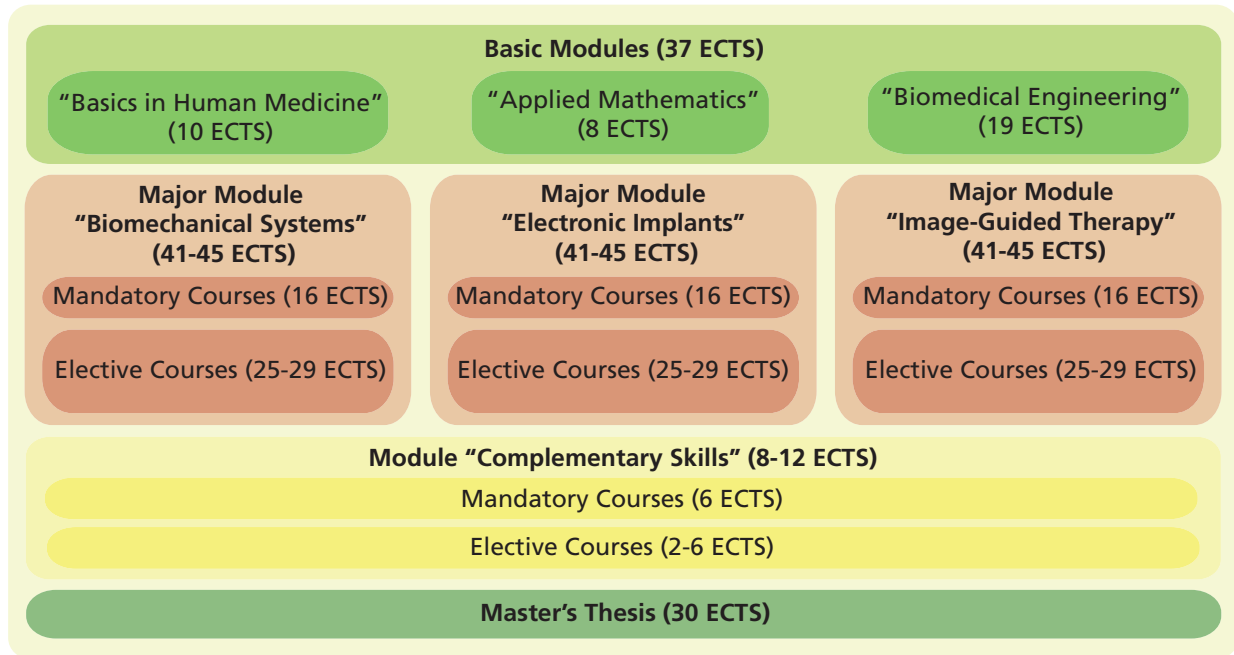
The choice of one of three major modules Biomechanical Systems, Electronic Implants, or Image-Guided Therapy after the first semester constitutes the first opportunity for specialization.

Approximately one third of the major modules consist of mandatory courses. In the elective part of the major module, the student is allowed to select every course from the list of courses in the master's program, giving rise to a high degree of diversity and flexibility and allowing for numerous course combinations. However, this freedom makes it somewhat difficult for the student to make reasonable choices regarding professional prospects.

This is why the responsible lecturers developed a recommended study plan to guide the students through the course selection process and to avoid organizational problems such as overlapping courses. If a student follows the recommended path, he or she can be sure to establish a sound professional profile.

### Module "Complementary Skills"

Apart from the rapid development of technology itself, today's biomedical engineers are increasingly challenged by complementary issues like ethical aspects, project planning, quality assurance and product safety, legal regulations and intellectual property rights, as well as marketing aspects. Language competence in English is of paramount importance both in an industrial and academic environment. This situation has been accounted for by the introduction of a new module called "Complementary Skills" where students are required to complete two mandatory courses (Innovation Management; Fundamentals of Quality Management and Regulatory Affairs) as well as 2–6 ECTS from the electives courses (Ethics in Biomedical Engineering; Scientific Writing in Biomedical Engineering; Clinical Epidemiology and Health Technology Assessment.)



### Master's Thesis

The last semester is dedicated to a master's thesis project on an individually suited topic in an academic research group at the University of Bern or the Bern University of Applied Sciences or, for particular cases, in an industrial research and development environment. As a rule, all 90 ECTS credits from the course program have to be completed, thus ensuring that the student is able to fully concentrate on the challenges imposed by exciting research activities. The master's thesis includes the thesis paper, a thesis presentation and defense as well as a one-page abstract for publication in the Annual Report of the master's program.

### List of Courses

- Advanced Topics in Machine Learning
- Applied Biomaterials
- Basics in Physiology for Biomedical Engineering
- Biological Principles of Human Medicine
- (Bio)Materials
- Biomechanics Labs
- Biomedical Acoustics and Audiology
- Biomedical Instrumentation
- Biomedical Laser Applications
- Biomedical Sensors
- Biomedical Signal Processing and Analysis
- BioMicrofluidics
- C++ Programming I
- C++ Programming II
- Cardiovascular Technology
- Clinical Applications of Image-Guided Therapy
- Clinical Epidemiology and Health Technology Assessment
- Computer-Assisted Surgery
- Computer Graphics
- Computer Vision
- Continuum Mechanics
- Design of Biomechanical Systems
- Dynamical Models: Analysis, Conception and Simulation
- Ethics in Biomedical Engineering
- Finite Element Analysis I
- Finite Element Analysis II
- Fluid Mechanics
- Functional Anatomy of the Locomotor Apparatus
- Fundamentals of Quality Management and Regulatory Affairs
- Image-Guided Therapy Lab
- Innovation Management
- Intelligent Implants and Surgical Instruments
- Introduction to Biomechanics
- Introduction to Digital Logic
- Introduction to Electrical Engineering
- Introduction to Engineering Mechanics
- Introduction to Medical Statistics
- Introduction to Programming
- Introduction to Signal and Image Processing
- Introductory Anatomy and Histology for Biomedical Engineers
- Lecture Series on Advanced Microscopy
- Low Power Microelectronics
- Machine Learning
- Medical Image Analysis
- Medical Image Analysis Lab
- Medical Informatics
- Medical Robotics
- Microsystems Engineering
- Numerical Methods
- Ophthalmic Technologies
- Orthopaedic Surgery – Practical Course
- Osteology
- Principles of Medical Imaging
- Programming of Microcontrollers
- Regenerative Dentistry for Biomedical Engineering
- Rehabilitation Technology I
- Rehabilitation Technology II
- Scientific Writing in Biomedical Engineering
- Selected Chapters in Mathematics
- Short Introduction to MATLAB
- Technology and Diabetes Management
- Tissue Biomechanics
- Tissue Biomechanics Lab
- Tissue Engineering
- Tissue Engineering - Practical Course
- Wireless Communication for Medical Devices

## Major Modules

### Biomechanical Systems



Prof. Dr. Philippe Zysset

The respiratory, cardiovascular and musculoskeletal systems are the transport and structural bases for our physical activities and their health have a profound influence on our quality of life. Lung diseases, cardiovascular diseases, musculoskeletal injuries and pathologies are costly ailments facing our health care systems, both in terms of direct medical costs and compensation payments related to loss-of-work.

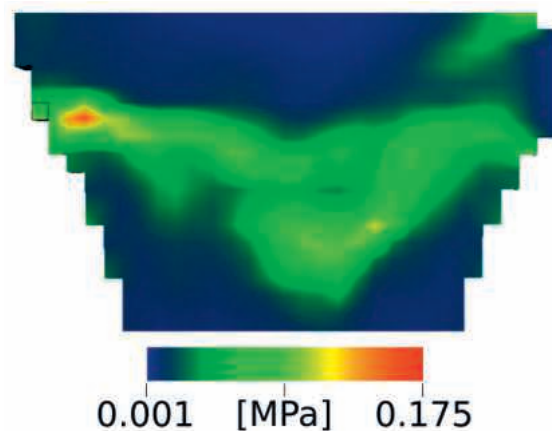
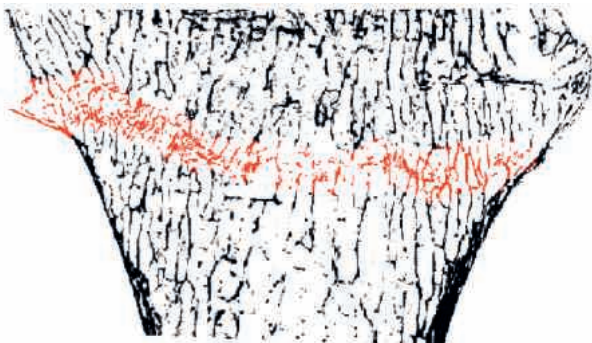
In this module, students will gain a comprehensive understanding of the multi-scale organisation of the respiratory, cardiovascular and musculoskeletal systems, combining knowledge from the cell, tissue, organ to the body level. They will learn how to apply engineering, biological and medical theory and methods to resolve complex problems in biomechanics and mechano-biology. Students will learn to draw connections between tissue morphology and mechanical response, and vice versa. Students will also gain the required expertise to apply their knowledge in relevant, practice-oriented problem solving in the fields of pneumology, cardiology, cardiovascular surgery, orthopaedics, dentistry, rehabilitation and sports sciences.

The mandatory courses in this module provide the student with fundamental knowledge of fluid and solid mechanics, tissue engineering, tissue biomechanics and finite element analysis. This provides an overview of the functional adaptation of the respiratory, cardiovascular or musculoskeletal system to the demands of daily living, and the necessary conditions for its repair and regeneration. This major module requires a prior knowledge of mechanics, numerical methods and related engineering sciences, as many of the mandatory and elective courses

build upon these foundations. Elective courses allow the students to extend their competence in a chosen direction, gaining knowledge in analytical methodologies, medical device design, minimally invasive surgery or rehabilitation.

Knowledge gained during the coursework highlights the multidisciplinary nature of this study focus area, encompassing the cell to body, the idea to application and the lab benchtop to the hospital bedside. This knowledge is applied during the final thesis project, a project often with a link to a final diagnostic or therapeutic application. Examples of recent master thesis projects include estimation of pulsatile flow with serial-section light microscopy, development of microfluidic systems for micro-vascularisation or optomechanical simulations of laser refractive surgeries.

Career prospects are numerous. Many students proceed to further post-graduate education and research, pursuing doctoral research in the fields of biomechanics, tissue engineering, lab on chip or development of biomaterials. Most of the major companies in the fields of cardiovascular technology, orthopaedics, dentistry, rehabilitation engineering and pharmaceuticals are strongly represented within the Swiss Medtech industry and have an ongoing demand for graduates of this major module. At the interface between biomedical engineering and clinical applications, graduates may also pursue careers related to the evaluation and validation of contemporary health technology, a cornerstone for future policies on the adoption of these new methods in the highly competitive health care domain.



Transverse fracture zone due to compression of the distal tibia. Experiment and coarse/fast simulation method.

# Major Modules

## Electronic Implants



Prof. Dr. Volker M. Koch

Electronic implants are devices like cardiac pacemakers and cochlear implants. Due to miniaturization and other developments, many new applications become feasible and this exciting area is growing rapidly. For example, cochlear implants provide already approximately more than 320'000 people worldwide a sense of sound. These people were previously profoundly deaf or severely hard of hearing. Recently, researchers demonstrated that electronic retinal implants allow the blind to read large words.

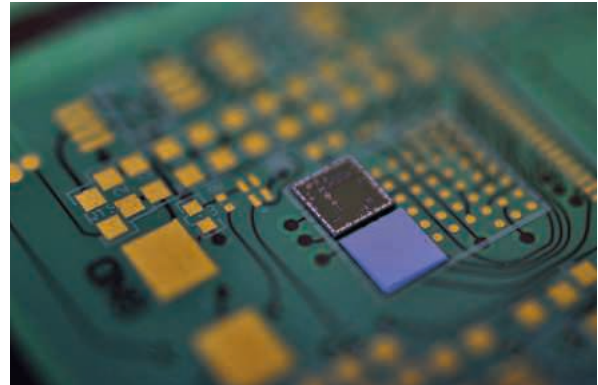
There are many more applications for electronic implants beyond treating heart problems, hearing loss or blindness. For example, there are electronic implants that treat Parkinson's disease, obesity, depression, incontinence, hydrocephalus, pain, paraplegia, and joint diseases.

In this module, students will gain a comprehensive technical and application-oriented understanding that will allow them to select, use, design, and optimize electronic implants and similar biomedical systems. Since the work on such complex systems is usually done in interdisciplinary groups, another important goal is that graduates are able to work and communicate in teams consisting of, e.g., engineers, scientists, and medical doctors.

Specifically, students will learn about technology basics including intelligent implants and surgical instruments, biomedical signal processing and analysis, low-power microelectronics, wireless communications for medical devices, and microsystems engineering including MEMS technology. Application-oriented elective courses are also taught, e.g., cardiovascular technology, biomedical sensors, biomedical acoustics, biomedical laser applications, ophthalmic technologies, and diabetes management.

Students may already apply their knowledge as a part-time assistant in an institute and/or during their master's projects. After finishing the degree program, a wide variety of career paths are available, ranging from research and development to project and product management. Many companies in Switzerland work in this field and "traditional" implants manufacturers have recently become interested in electronic implants, e.g., to measure forces in knee implants.

This major is open to all students of our master's program. However, typically, students have an engineering-related background, for example, electrical engineering, microtechnology engineering, systems engineering, mechatronics engineering, mechanical engineering, or computer science.



ECG recorder using a liquid crystal polymer (LCP) with two ASIC chips, developed at BFH.



Electrophysiologic catheter using a liquid crystal polymer (LCP) and thermoplastic polyurethane (TPU).

## Major Modules

### Image-Guided Therapy



Prof. Dr. Stefan Weber

Image-Guided Therapy refers to the concept of guiding medical procedures and interventions through perceiving and viewing of medical image data, possibly extended by using stereotactic tracking systems. Medical imaging typically relates to a great variety of modalities ranging from 2D fluoroscopy and ultrasound to 3D computed tomography and magnet-resonance imaging, possibly extended to complex 4D time series and enhanced with functional information (PET, SPECT). Guidance is realized by determination of the spatial instrument-to-patient relationship and by suitable visualization of tracking and medical image data. Image guidance is very often accompanied by other surgical technologies such as surgical robotics, sensor enhanced instrument systems as well as information and communication technology.

Students of the IGT module will study the clinical and technical fundamentals of image-guided therapy systems. They will develop an understanding of currently applied

clinical standards as well as an overview of latest advancements in research. Successful students will be enabled to develop novel clinic-technological applications for complex medical procedures as well as improve existing approaches. This will be the basement for successful careers both in the industrial and academic sector.

Mandatory courses of this module are concerned with the fundamentals of Signal and Image Processing and Medical Image Analysis. Furthermore, fundamental aspects of stereotactic image guidance, tracking, patient-to-image registration and basic clinical applications are taught in the course Computer-Assisted Surgery. Recent trends and fundamental aspects in surgical robot technology, minimally invasive procedures and its applications within IGT are introduced in the course Medical Robotics. Additional elective courses extend students competencies in related areas such as computer graphics, pattern recognition, machine learning, and regulatory affairs.

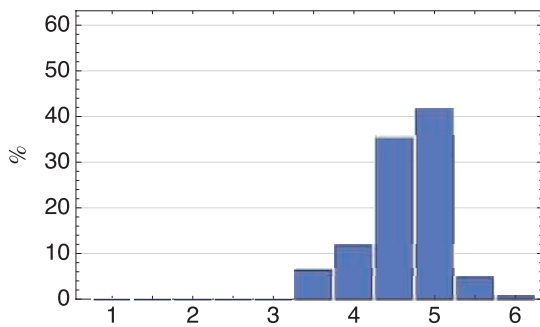


Engineers in discussion with a physician regarding work space requirements of robotic-assisted spinal surgery platform.  
© university 2020

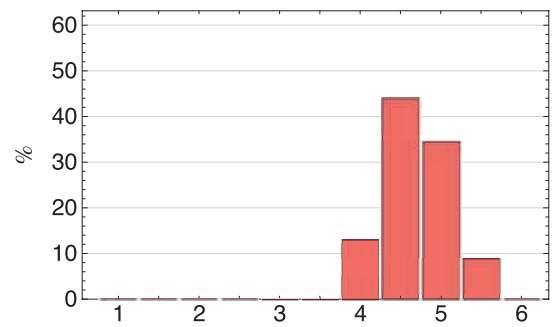
## Evaluation of Courses in the Year 2020

Like in the previous years, a centralized online evaluation was performed in the master's program in Spring and Fall Semester 2020 according to the guidelines of the University of Bern. Both semesters were considered leading to 53 course evaluations involving 831 forms in total. The results regarding all forms (see below) reveal that despite the difficulties associated with the pandemic situation, the students are generally satisfied with the program and that the courses are interesting and promote the acquisition of skills.

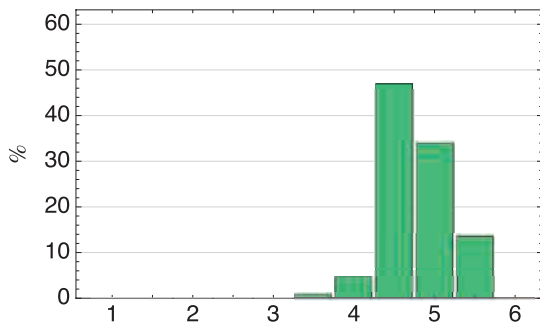
Increase of Interest



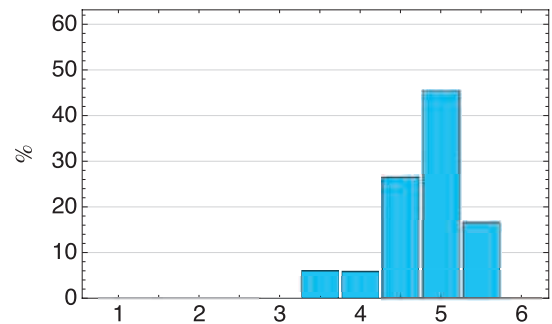
Acquisition of Cognitive Skills



Acquisition of Motivational Skills



Satisfaction



## Hard Work Pays off: The RMS Award



Michel Hayoz

In 2020, the RMS Award went to Michel Hayoz for his excellent GPA of 5.89/6.0.

In his thesis „Stereo-Endoscope to CT Image Data Registration for Liver Surgery“ he proposed a non-rigid registration method for image-guided laparoscopic liver surgery to reconstruct an intra-operative liver model from a stereoscopic video stream frame by frame. Michael Hayoz is working as computer scientist in the ARTORG Artificial Intelligence in Medical Imaging lab.

The RMS Award is an award of excellence. Each year, the Robert Mathys Stiftung (RMS), an independent service

laboratory and research institute, gives it to the best BME student for his/her outstanding achievements.

The award of 1000 CHF honors the student who receives the best grade point average over the course of the two-year BME master's program.

The study direction wishes to thank Dr. Beat Gasser and the executive board of the Robert Mathys Foundation for this contribution to the excellence and visibility of our biomedical engineering field.

## Faculty

### University of Bern

Christiane Albrecht, Prof. Dr.  
Mariya Asparuhova, Dr.  
Tommy Baumann, Dr.  
Claus Beisbart, Prof. Dr.  
Julia Bohlius, PD Dr.  
David Bommès, Prof. Dr.  
Dieter Bosshardt, Prof. Dr.  
Philippe Büchler, Prof. Dr.  
Jürgen Burger, Prof. Dr.  
Ramona Buser, Dr.  
Roch-Philippe Charles, PD Dr.  
Marcel Egger, Prof. Dr.  
Sigrun Eick, Prof. Dr.  
Paolo Favaro, Prof. Dr.  
Cristian Fernández Palomo Dr.  
Martin Frenz, Prof. Dr.  
Benjamin Gantenbein, Prof. Dr.  
Amiq Gazdhar, PD Dr.  
Kate Gerber, Dr.  
Nicolas Gerber, Dr.  
Nikolaos Gkantidis, PD Dr.  
Olivier Guenat, Prof. Dr.  
Julien Paul Guerrero, Dr.  
Martin Hofmann  
Wilhelm Hofstetter, Prof. Dr.  
Samira Helena João de Souza, Dr.  
Joannis Katsoulis, Prof. Dr.  
Sonja Kleinlogel, Prof. Dr.  
Samuel Knobel  
Doris Kopp  
Jan Kucera, Prof. Dr.  
Ruth Lyck, Prof. Dr.  
Ange Maguy, PD Dr.  
Laura Marchal-Crespo, Prof. Dr.  
Ines Marques, Dr.  
Beatrice Minder  
Stavroula Mougiakakou, Prof. Dr.  
Tobias Nef, Prof. Dr.  
Dominik Obrist, Prof. Dr.  
Iwan Paolucci  
Ludovica Parisi, Dr.  
Jean Pascal Pfister, PD Dr.  
Clemens Raabe, Dr.  
Mauricio Reyes, Prof. Dr.  
Anne Rutjes, Dr.  
Thiago Saads Carvalho, PD Dr.  
Shankar Sachidhanandam, PD Dr.  
Ekaterina Safroneeva, PD Dr.  
Narayan Schütz  
Walter Martin Senn, Prof. Dr.

Adrian Spörri, Dr.  
Alexandra Beatrice Stähli, Dr.  
Hubert Steinke, Prof. Dr.  
Jürg Streit, Prof. Dr.  
Raphael Sznitman, Prof. Dr.  
Prabitha Urwyler, PD Dr.  
Stefan Weber, Prof. Dr.  
Wilhelm Wimmer, Dr.  
Thomas Wyss Balmer, Dr.  
Soheila Zeinali, Dr.  
Marcel Zwahlen, Prof. Dr.  
Philippe Zysset, Prof. Dr.

### Bern University Hospital (Inselspital)

Daniel Aeberli, Prof. Dr.  
Stefano De Marchi, PD Dr. med.  
Rainer Egli, Dr.  
Andreas Häberlin, PD Dr.  
Hansjörg Jenni  
Alexander Kadner, Prof. Dr.  
Martin Kompis, Prof. Dr.  
Hubert Kössler  
Thomas Küffer  
Vladimir Makaloski, PD Dr. med.  
Rouven Porz, Prof. Dr.  
Lorenz Räber, Prof. Dr.  
Nikola Saulacic, PD Dr. med.  
Michael Schär, Dr. med.  
Kuangyu Shi, PD Dr.  
Waldo Valenzuela, Dr.  
Roland Wiest, Prof. Dr.

### Bern University of Applied Sciences

Partrik Arnold, Prof. Dr.  
Christof Baeriswyl  
Norman Urs Baier, Prof. Dr.  
Heiner Baur, Prof. Dr.  
Bertrand Dutoit, Prof. Dr.  
Patric Eichelberger, Dr.  
Juan Fang, Dr.  
Laëtitia Galea, Dr.  
Andreas Habegger, Prof.  
Kenneth James Hunt, Prof. Dr.  
Marcel Jacomet, Prof. Dr.  
Jörn Justiz, Prof. Dr.  
Theo Kluter, Prof. Dr.  
Volker M. Koch, Prof. Dr.  
Martin Kucera, Prof.  
André Lisibach, Prof. Dr.  
Alexander Mack, Dr.

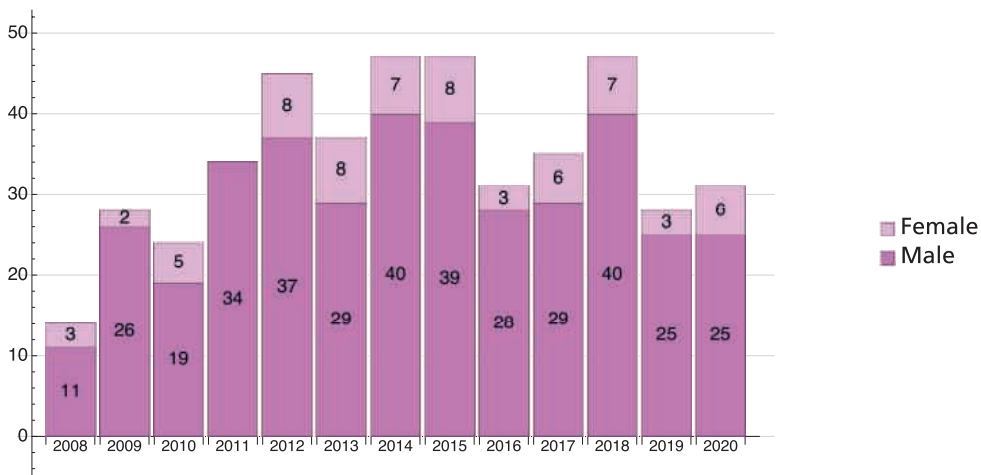
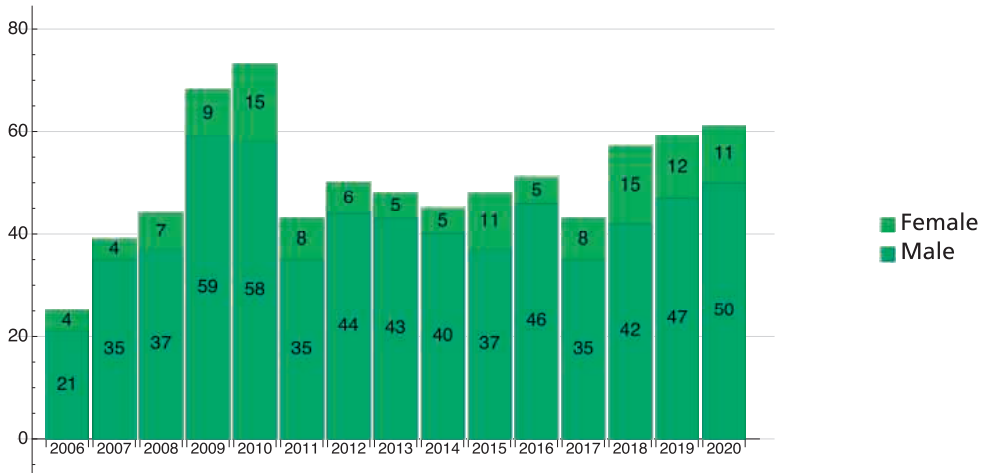
Christoph Meier, Prof.  
Thomas Niederhauser, Prof. Dr.  
Stefan Schmid, Dr.  
Patrick Schwaller, Prof. Dr.  
Andreas Stahel, Prof. Dr.  
Jasmin Wandel, Prof. Dr.

### Partner Institutions and Industry

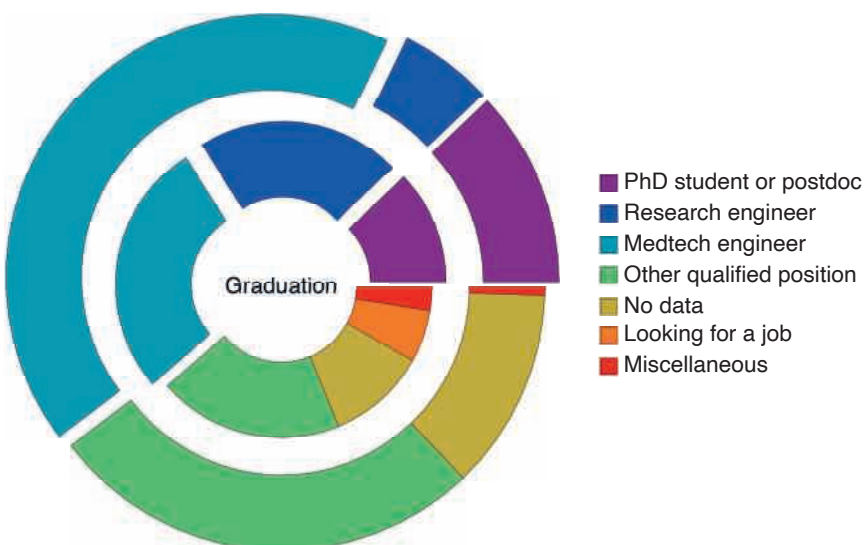
Markus Angst, Dr.  
Markus Auly  
Alessandro Bertolo, Dr.  
Marc Bohner, Prof. Dr.  
Emmanuel de Haller, Dr.  
Nicolas Alexander Diehm, Prof. Dr.  
Nicola Döbelin, Dr.  
Alex Dommann, Prof. Dr.  
Stefan Eggli, Prof. Dr.  
David Eglin, Dr.  
Lukas Eschbach, Dr.  
Marie-Noëlle Giraud, PD Dr.  
Daniel Haschtmann, PD Dr.  
Bernd Heinlein, Prof. Dr.  
Philipp Henle, Dr. med.  
Roman Heuberger, Dr.  
Ulrich Hofer, Dr.  
Thomas Imwinkelried, Dr.  
Björn Jensen, Dr.  
Gerhard Kirmse, Dr.  
Mark Kleinschmidt, Dr.  
Jens H. Kowal, PD Dr.  
Beat Lechmann  
Reto Lerf, Dr.  
Reto Luginbühl, Dr.  
Katharina Maniura, Dr.  
Simon Milligan, Dr.  
Walter Moser, Dr.  
Benjamin Pippenger, Dr.  
Felix Reinert, Dr.  
Simone Rizzi, Dr.  
Barbara Rothen-Rutishauser, Prof. Dr.  
Birgit Schäfer, PD Dr.  
Adrian Schneider, Dr.  
Matthias Schwenkglens, Prof. Dr.  
Jivko Stoyanov, PD Dr.  
Tim Vanbellingen, Dr.  
Peter Varga, Dr.  
Peter Wahl, Dr. med.  
André Weber, Dr.  
Tobias Wyss, Dr.  
Andreas Zumbühl, Prof. Dr.

## Statistics

### Number of New Students (above) and Graduates (below)



### Profession after Graduation: Activity after 1 and 5 years



The professional activity of our alumni one (inside) and five years (outside) after graduation (data 2015-2020).

## Graduate Profile Britton Marlatt



First week of classes at Hauptgebäude (September 2018)



Hiking with ARTORG colleagues in Valais (August 2020)

**Q:** What was your academic and professional background prior to your BME studies?

**A:** I completed my bachelor's degree in biomedical engineering at the University of Texas at Austin in 2016. While pursuing my bachelor's degree, I was concurrently employed as an engineer at a biotech startup in Austin, Texas. Subsequently, I worked in technology consulting on largescale software implementations for two years before matriculating at the University of Bern for the master's program.

**Q:** Why did you choose to pursue your Master's studies at the University of Bern/Bern University of Applied Sciences?

**A:** I wanted to pursue further education in applied machine learning in the medical field, and the University of Bern offers tremendous academic opportunities in this discipline via the master's program in biomedical engineering. Artificial intelligence as a subject matter is very interesting and I thought this degree would be foundational for me in pursuing a career in this industry. Additionally, the master's program offers specialized major modules, and the Image-Guided Therapy option provides coursework that interested me, including machine learning, computer vision and medical image analysis, which drew me to this particular specialization within the master's program.

**Q:** You continued to work during your studies. How was this experience?

**A:** During my last two semesters I was able to work as a graduate research assistant at the ARTORG Center for Biomedical Engineering. Specifically, I was blessed to work with Prof. Dr. Raphael Sznitman and Dr. Márquez-Neila in the Artificial Intelligence in Medical Imaging Department. This experience complemented my studies well, and allowed me to dive deeper into certain subjects from my coursework and apply machine learning concepts to real world medical datasets. I also particularly valued the comradery within the lab group, and the availability to ask questions and learn from the postdocs and PhD students. We routinely ate lunch together and went on team outings like curling in Bern and hiking in the Alps.

**Q:** What was your career plan after the completion of your degree/Where do you work now?

**A:** While completing my thesis, I was also heavily occupied with job applications in both Switzerland and the United States. Despite the challenges that Covid presented while seeking employment opportunities, I was happy to accept an offer as a Senior Data Scientist at InformAI, Inc. in Houston, Texas, which began one month after graduation. I work with leading physicians from various medical institutions within the Texas Medical Center in discovering associations in their data to create novel medical image classification and patient outcome prediction algorithms, and bring them to market. Upon arriving my first day, I was surprised to learn how large the Texas Medical Center is. Covering 5.4 km<sup>2</sup>, it is the largest medical complex in the world with a surgery performed once every three minutes on average. The sheer amount of data and medical records produced from such institutions is staggering, and makes Houston an exciting place for translational research and biomedical innovation.

**Q:** What is the benefit of the Master studies with regard to your current professional activity?

**A:** I am very pleased with how well the master's degree program prepared me for my current occupation. In many ways, my job feels like a pleasant continuation of what I studied in Bern. Not only was I exposed to various applied medical imaging and machine learning concepts, but I was also introduced to regulatory affairs. As my research projects progress towards commercialization, it is important to have an understanding of medical device regulations in the U.S., Europe and abroad. I also learned many valuable lessons from the master thesis process such as long-form technical writing, experimental design and troubleshooting challenging obstacles on the fly. My experience studying at the University of Bern has given me invaluable knowledge, contacts and confidence in this industry.

# The Biomedical Engineering Club

## The BME Club and Its Mission

The Biomedical Engineering (BME) Club is a non-profit alumni organisation from the University of Bern that aims to provide and promote networking events among its interdisciplinary members. We are a constantly growing group of biomedical engineers, scientists, past and present students and medical technology corporate eager to bring together the fields of engineering, biology, and clinical medicine. The BME-Club accomplishes these goals by networking and hosting events, in particular, information sessions to learn about cutting-edge research fields of bioengineering, attendance of national/international conferences, and visit plans to industries and laboratories. The BME Club has been recognized as an official alumni association of the University of Bern under the umbrella organization – Alumni UniBE. A dedicated executive committee within the BME Club follows the principles of our constitution. We are an enthusiastic and versatile group that performs diverse activities including:

- Regular visits to Swiss medical and engineering companies
- Organization of the annual MEDICA trip
- Information on career opportunities for Masters levels
- Organization of the annual welcome event for new students of the BME Master program
- Organization of an annual alumni gathering for networking purposes
- Sponsorship of the Best Master's Thesis Award at the annual BME Day
- Sponsorship of 2 travel grants to international conferences
- Joint membership for former students of the University of Bern
- Offering (optional) joint membership with Swiss Society for Biomedical Engineering

Taken together, the BME Club represents a unique platform for professional, lifelong communication and networking events. Further details on the BME Club are available in our website [www.bmeclub.ch](http://www.bmeclub.ch).

## How to Join

Becoming a BME member is easy! Simply join any BME Club event or sign in at our website. We are looking forward to seeing you.

## BME Club on Pause

Due to the current pandemic situation in Switzerland and worldwide, we had to cancel all of our planned events. Despite the cancellation of the BME Day 2020, we are very happy to announce the Best Master's Thesis Award winner Ms. Giuditta Thoma. Her thesis entitled "Lung-Alveoli-on-Chip: Mechanical Characterization of a New Biological Membrane" has been awarded 300 CHF.

We hope for more visit possibilities and networking events in 2021 and are supporting the BME Master's course in the organization of the next virtual BME Day 2021.

## The BME Club Board in 2020



Samuel Knobel  
**President**  
M.Sc. class 2016



Tamara Melle  
**Secretary, Treasurer**  
M.Sc. class 2017



Adel Tekari  
**Alumni Representative**  
M.Sc. class 2007



Mark Keller  
**Corporate Representative**  
M.Sc. class 2007



Tobias Imfeld  
**Webmaster**  
M.Sc. class 2009



Fredrick Joseph  
**PhD Student Representative**



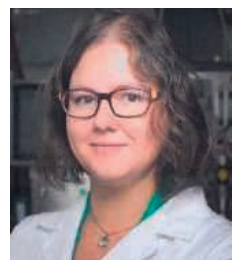
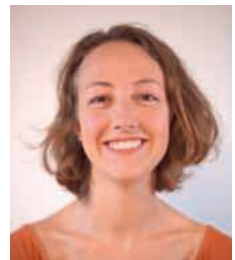
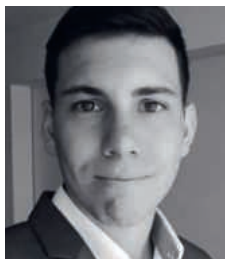
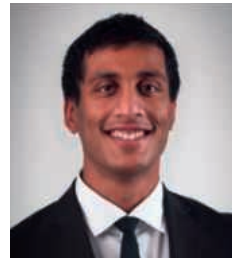
BME Club campus tour for new students



Giuditta Thoma



MASTER'S THESES  
2020



# Evaluation of Respiratory Influences on Pulmonary Artery Pressure (PAP) to Analyze PAP-Measurements in Cardiac Insufficiency

Kay S. Ackermann



Supervisors: Prof. Dr. Thomas Niederhauser, Dr. Olaf Skerl  
Institutions: Bern University of Applied Sciences, Institute for Human Centered Engineering  
Biotronik SE & CO. KG, Berlin  
Examiners: Prof. Dr. Jürgen Burger, PD Dr. med Dr. phil. Andreas Häberlin

## Introduction

Cardiac insufficiency, more commonly known as heart failure (HF), is one of the leading and still growing chronic diseases. Continuous progression of the disease can lead to cardiac decompensation and may require intensive care medicine. The development of a typical decompensation is accompanied by an increase in pulmonary artery pressure (PAP). With monitoring the PAP, a decompensation can be detected early, and therapeutic actions for prevention can be initiated. This reduces HF hospitalization, including their costs, improves the survival of the patients, and finally, the quality of life among HF patients. However, the PAP is modified and superimposed by many physiological conditions. Therefore, especially in few, infrequently, and time-limited recordings, these influences must be minimized for a proper diagnosis. The location of the PA in the intrapleural cavity evolves the hypothesis that the respiration influences the PAP significantly and was examined in detail in this thesis.

## Materials and Methods

For robust statements, all PAP influences were examined while focusing on respiratory influences. Due to complexity, this examination was mainly limited to healthy, resting humans. The lack of PAP-synchronized respiratory measurements requires the development of novel methods to directly separate the respiration from the PAP for respiratory analysis. After successful separation, different approaches to minimize the PAP's respiratory modulation were developed and applied. For these procedures, 14 PAP measurements of 30 seconds were selected from five healthy sheep on pasture or in a barn.

## Results

By literature research, the intrapleural pressure (IP) was identified to be the primary modulator on the

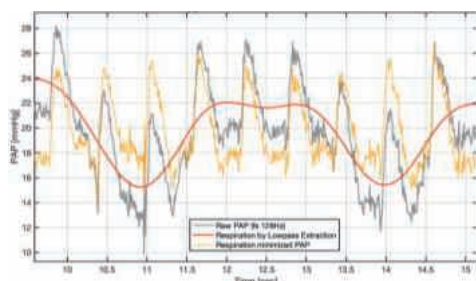


Fig. 1 PAP (grey) with extracted respiratory modulation (red) and respiratory modulation minimized PAP (yellow).

PAP, which acts directly through the PA wall. The respiratory modulations of PAP were found to be significant of 4-5 mmHg in healthy humans in rest, where the PAP rises during expiration and falls in inspiration. During forced respiration, the modulations can increase over 10 mmHg. The transferability of discoveries found in sheep data to human was examined and confirmed. It was found that respiratory minimization by subtraction of the respiration directly extracted out of the PAP is an option (Fig.1), but producing a high effort in signal processing and sensitivity to artefacts. Another approach uses the periodic properties of respiration, which neutralize itself statistically in time in a Sinc(t) manner. Finally, to reduce the error on mean PAP parameters coming from respiration to less than 1 mmHg, a PAP measurement needs to include at least 3 respiratory cycles (Fig.2) in healthy resting subjects. This implies a PAP snippet duration of 21 seconds in a worst-case scenario, including a respiratory cycle duration of 7 seconds.

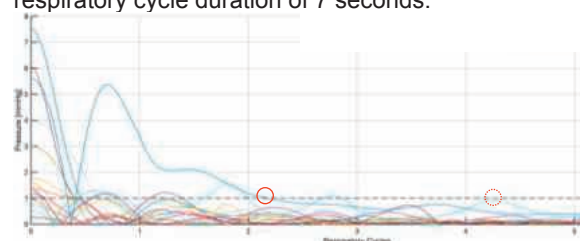


Fig. 2 Absolute error on the mean PAP parameter due to respiratory modulation from 14 PAP snippets.

## Discussion

The results correspond to cardiology statements, where the respiratory influence is significant and should neutralize itself after averaging over a few respiratory cycles. However, the low number of evaluated measurements require verifying results by a larger dataset. Overall, the thesis developed a part of the essential basics to understand the PAP behaviour and its signal processing to diagnose an impending decompensation in an early stage.

## References

D. P. Zipes, et al., Braunwald's Heart Disease, A Textbook of Cardiovascular Medicine, 11 ed. Elsevier Health Sciences, p.403-405, 2018.

## Acknowledgements

A special thanks to Prof. Jürgen Burger and Biotronik Berlin to enable this international cooperation of the academic field and the medical industry.

# Estimating Pulsatile Flow via Analysis of Serial-Section Light-Sheet Microscopy

Léonard Barras



Supervisors: Prof. Dr. Dominik Obrist, Dr. Michael Liebling  
Institutions: University of Bern, ARTORG Center  
IDIAP Research Institute  
Examiners: Prof. Dr. Dominik Obrist, Dr. Michael Liebling

## Introduction

Pulsatile flow plays an important role during development of the vertebrate circulatory system, in particular, the heart. The variation of direction and the high velocities make difficult to quantify them. Optical sectioning microscopy offers the possibility of imaging sections within developing embryos or larvae of animal models such as the zebrafish at high speed. The flows studied in vivo evolve over time and the different biological samples. Video stacks at high spatial resolution cannot be recorded simultaneously. Several techniques have been proposed that build upon the assumption of a repetitive flow to record rapid images series at different depths and, possibly orientations. A periodic synthetic flow would allow to record multiple periods and combined the measurements.

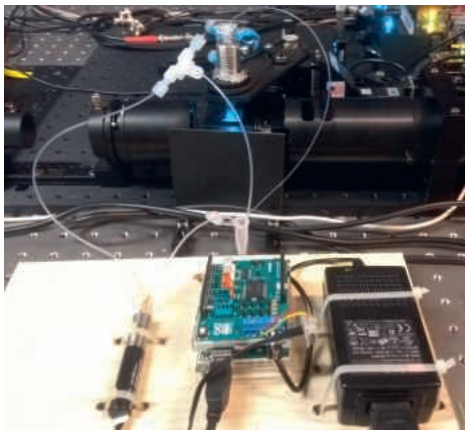


Figure 1 Experimental setup built to create a flow object observable with a light-sheet microscope

## Materials/Method

A synthetic pulsatile flow object which can be imaged under an existing light-sheet microscope has been created using a commercial pumping system and FEP tubing. Fluorescent beads have been mixed with the fluid for allowing its quantification with Particle Image Velocimetry (PIV) algorithms. The flow object was mounted on a 4D motorized stage, allowing its displacement in the laser sheet.

## Results

Experiments showed the challenges of creating a microscale synthetic flow at velocities allowing its quantification with a camera. High velocities induce large displacement of the tracer particles making difficult to apply standard PIV algorithms. The fluidic circuit was adjusted until a quantifiable flow were obtained. A method was proposed to register multi angles video stacks.

## Discussion

Video stacks have been acquired under different orientations. The flow could be analyzed with the light sheet microscope and quantified with PIV algorithms. The velocity analysis allowed the characterization of the system and the flow.

## References

Pitrone et al. Nature Methods, 2013 DOI:  
10.1038/nmeth.2507  
Chan and Liebling, ISBI'2015 DOI:  
10.1109/ISBI.2015.7163893

## Acknowledgements

I would like to thank Prof. Dominik Obrist for having accepted to supervise my thesis and the group of Dr. Michael Liebling at the IDIAP Research Institute.

# Investigation of the Contribution of SHIP1 and Immune Cells to Bone Cell Lineages

Margaux Bringardner



Supervisors: Prof. Dr. Willy Hofstetter, PD Dr. Philippe Krebs  
Institution: University of Bern, Department for BioMedical Research  
Examiners: Prof. Dr. Willy Hofstetter, PD Dr. Philippe Krebs

## Introduction

Bone cell lineages and immune cells communicate with each other and are closely related. They release different factors influencing one another.

Previous research in the lab showed that inositol polyphosphate-5-phosphatase D (SHIP1 or Styx) KO (knock-out) mice have osteoporosis phenotype. SHIP1 is a pseudo-phosphatase regulating osteoclast progenitor cells (OPC) differentiation, proliferation, and survival through CSF-1 or RANKL signalling pathway. Another study in the lab showed that TKO (triple knock-out,  $Styx^{-/-}$ ,  $Rag2^{-/-}$ ,  $\gamma C^{-/-}$ ) recovers the loss of bone density to the wild type (wt) level. Recombination Activating 2 ( $Rag2$ ) is an accessory factor for the maturation of B and T cells, while  $\gamma C$  is a common subunit of several interleukin receptors important for proliferation, differentiation, and survival of lymphocytes.

The aim of this project was to investigate the underlying mechanisms leading to osteoporosis in Styx KO mice, and to the recovering of osteoporosis in TKO mice.

## Materials and Methods

To evaluate osteoclast (OC) development of Styx KO mice *in vitro*, OPC from Styx KO, Styx het. (heterozygous) and wt mice were grown for 6 days with different concentration of RANKL, and 30 ng/ml of CSF-1. Micro computed tomography (micro-CT) of vertebra and distal femur were performed to evaluate bone structure.

OPC from TKO ( $Styx^{-/-}$ ,  $Rag2^{-/-}$ ,  $\gamma C^{-/-}$ ), DKO Styx het. ( $Styx^{+/+}$ ,  $Rag2^{-/-}$ ,  $\gamma C^{-/-}$ ), and DKO Styx wt (double knock-out,  $Styx^{+/+}$ ,  $Rag2^{-/-}$ ,  $\gamma C^{-/-}$ ) mice were grown in the same conditions as above. Osteoblasts (OB) from wt mice were cultured with a titration of SHIP1 inhibitor and either BMP2 or  $1,25(OH)_2D$ .

XTT (cell viability assay), TRAP activity and qRT-PCR for OC gene markers were performed to investigate OC development. Mineral dissolution capacity of OC was evaluated by culturing the OC on calcium phosphate (CaP) spiked with  $^{45}Ca$ , and measuring the released  $^{45}Ca$  in the supernatant.

## Results

Cell viability and differentiation assays revealed that OPC from Styx KO and TKO mice had less TRAP activity per XTT than wt OPC (day 6: mean decrease of 40% for Styx KO and 70% for TKO). Calcium resorption measurements demonstrated less

resorption for Styx KO and TKO. In contrast, vertebrae and distal end of femora from Styx KO mice showed osteoporotic phenotype (-39.6% BV/TV), but not TKO bones (Fig. 1). Experiments with SHIP1 inhibitor and OB showed that XTT values decreased significantly from 8.5 to 10.5 nM of SHIP1 inhibitor. Already concentration of 6.25 nM SHIP1 inhibitor impaired the OPC differentiation.

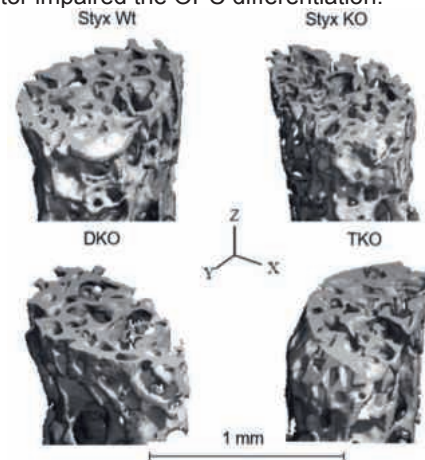


Fig. 1: Micro-CT of vertebra (L3) of Wild type, Styx KO,  $Rag2 + \gamma C$  KO, and Styx +  $Rag2 + \gamma C$  KO. Osteoporosis phenotype is observable in Styx KO bone (-39.6% bone density compared to Wt).

## Discussion

OPC from Styx KO mice exerted less osteoclastogenic potential compared to the wt mice. Furthermore, OC from Styx KO mice showed less OC activity. However, when an immunodeficiency is added through  $Rag2^{-/-}$  and  $\gamma C^{-/-}$ , impaired bone resorption and formation are compensated and the osteoporotic phenotype is recovered. In OB, blocking SHIP1 decreased the cell viability and differentiation. The effect of SHIP1 on OB activity and function has yet to be elucidated.

## References

- Mark C Horowitz and al. How B cells influence bone biology in health and disease. *Bone*, 47(3):472–479, 2010. ISSN 8756-3282.
- Stephanie R Pulliam and al. Common gamma chain cytokines in combinatorial immune strategies against cancer. *Immunology letters*, 169:61–72, jan 2016. ISSN 1879-054

# Investigation of Corneal Lamellar Resections

Tim Büsch



Supervisors: Prof. Christoph Meier, MSc Niklaus Vogel  
Institutions: Bern University of Applied Sciences, Institute for Human Centred Engineering HuCE-optoLab  
Ziemer Ophthalmic Systems AG  
Examiners: Prof. Christoph Meier, MSc Niklaus Vogel

## Introduction

Lasers are widely spread in medicine, especially in ophthalmology. Two application examples are Optical Coherence Tomography (OCT) for diagnostics and femtosecond lasers for different treatments and surgeries. OCT is a non-contact imaging technique based on interferometry of low coherent light. Femtosecond lasers release powerful short pulsed bursts to cut and vaporize tissue. To investigate the performance of femtosecond lasers when applied for corneal lamellar resections, a measurement method is developed. Corneal tissue of a pig eye is resected and a volume scan of the treatment is acquired by a high-resolution OCT system. With an image processing algorithm the resection in the tissue is detected. Interpolations enable the calculation of the geometrics of the resection and allow a conclusion on the effects applied by the laser on the tissue.

## Materials and Methods

The used resection laser is a commercially available and clinical proven femtosecond laser system. It is in use for various eye treatments all over the world. The OCT system is made in the HuCE-optoLab and its outstanding feature is the high axial resolution. The large bandwidth of the laser source and a custom-made spectrometer are the main components which enable this feature.

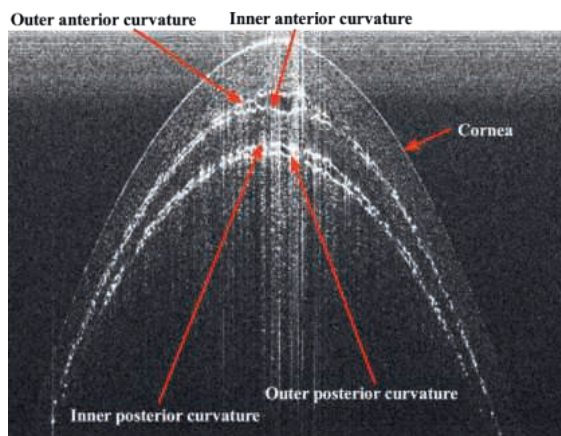


Fig. 1 One slice of the volume scan. Marked are the cornea and the four curvatures of the resection.

The detection algorithm is developed based on canny edge detection and k-means clustering. The edge detection is applied on a slice of the volume

scan (Fig.1) and the clustering on the whole volume. This enhances the robustness of the clustering. The clustered data points are interpolated by for example Zernike polynomials to obtain surfaces of the resections.

## Results

The developed measurement procedure and detection algorithm enable to detect the corneal resections applied in the tissue with a laser. With the different interpolation methods, the user can extract the dimensional informations he requests. As an example, a cubic spline interpolated thickness map of a resected part of the tissue is presented:

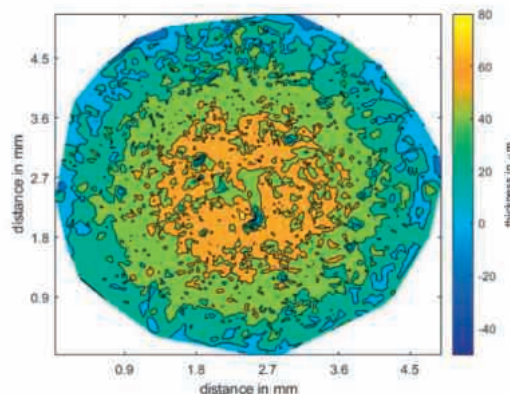


Fig. 2 Result of the detection algorithm presented as an interpolated thickness map of the resected tissue.

## Discussion

The measurement and detection procedure are a basis to verify the geometrics of corneal lamellar resections. Its advantages are the reliable detection of resections and the possibility to extend it with additional functions, depending on the demanding informations.

## References

Bakaraju, R. C., Ehrmann, K., Papas, E., & Ho, A. (2008). Finite schematic eye models and their accuracy to in-vivo data, 48, 1681–1694. <https://doi.org/10.1016/j.visres.2008.04.009>.

## Acknowledgements

Thanks to my supervisor Prof. Christoph Meier and the company Ziemer Ophthalmic Systems AG for their continuous support and helpful advice.

# Augmentation of OCT Biomarker Detection with Sparse Labels

Kevin Ceni

Supervisors: Prof. Dr. Raphael Sznitman, Thomas Kurmann  
Institutions: University of Bern, ARTORG Center for Biomedical Engineering Research  
Examiners: Prof. Dr. Raphael Sznitman, Dr. Pablo Márquez Neila



## Introduction

Optical Coherence Tomography (OCT) imaging is one of the most important imaging modalities in ophthalmology. One reason for its importance is due to its ability to image volumetric information of the retina in a fast, safe and cheap way, in order to diagnose pathologies. Age-related Macular Degeneration (AMD) and Diabetic Macular Edema (DME) are diseases which deform the retinal layers by the formation of fluids as the pathology progresses. Those fluids or deformations in the retinal layers are identified by clinicians as biological markers (biomarkers). Since the classification and localization of the biomarkers is a time-consuming and error-prone task, the aim of this project was to develop automated algorithms to detect and locate 10 different biomarkers in OCT volumes.

## Materials and Methods

The classification of the biomarkers was implemented using the support of Convolutional Neural Network (CNN). Three different types of CNN have been compared; Resnet [1], Wide Resnet [2] and Dilated Residual Network [3]. We employ two datasets for training and one for testing our proposed approaches.

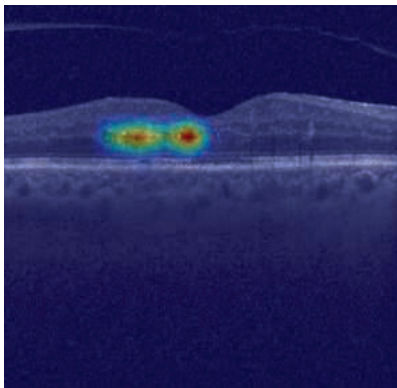


Fig. 1 Grad-CAM showing the Intraretinal Fluid (IRF) biomarker in a BScan, which is extracted from a OCT volume

The localization of biological markers is represented by three different methods. The first method uses the Gradient-weighted Class Activation Mapping (Grad-CAM) principle to determine where the biomarker is located in an OCT volume. The second method aims at covering part of the BScan to be analyzed to find

the correct position of the biomarker. The last method for localizing biomarkers is based on the concept of a moving window. The last part of the thesis aims at adding the possibility to detect new biological markers using data that only contains annotations for the new biomarkers.

The evaluation of the outcomes is done by comparing the average precision, sensitivity, specificity and area under the curve (AUC) between the methods.

## Results

The best performing CNN used for the classification of biomarkers is the Resnet [1]. The Area Under the Curve achieved on the classification of 10 biomarkers is of 94.7%. Considering the localization of biological markers task, the best performing algorithm is the one which apply a specific mask to each BScan. The average precisions achieved on it for the Subretinal Fluid (SRF) and Intraretinal Fluid (IRF) biomarkers are 86.7% and 99.1%, respectively. The overall average precision obtained when new biomarkers are added to the existing classifier is less than 50%.

## Discussion

These results obtained for the classification of biomarkers are promising. They showed that using an approach based on the usage of CNNs is a feasible solution to apply autonomous classification. The localization of biomarkers showed overall good performance. However, some limitations are given by the quality of the classifier, since it is strongly used to detect the presence of the biomarkers in a BScan. The performance obtained on the classification of new biomarkers showed that this is not an effective solution. Other approaches should be investigated.

## References

- [1] He K. et al., Deep Residual Learning for Image Recognition, CVPR, 2015.
- [2] Zagoruyko S. and Komodakis N., Wide Residual Networks, CoRR, 2016.
- [3] Fisher Y., Vladlen K and Funkhouser T. A., Dilated Residual Networks, CVPR, 2017.

## Acknowledgements

The continuous support of the ARTORG group of Artificial Intelligence in Medical Imaging is gratefully acknowledged.

# Estimation of the Energy Loss through Turbulence in an Aortic Stenosis Model using Backlight Particle Tracking Velocimetry in a Silicone Ascending Aorta Phantom

Maxime Chiarelli

Supervisor: Dr. med. Eric Buffle  
Institution: University of Bern, ARTORG Center for Biomedical Engineering Research  
Examiners: Prof. Dr. Dominik Obrist, Dr. med. Eric Buffle



## Introduction

Old patients suffering from aortic stenosis generally present a calcified, tricuspid aortic valve. The calcification of the aortic valve is associated with an increase in the leaflet stiffness and a narrowed valve orifice which increase the transvalvular pressure gradient across the aortic valve. Echocardiography is the gold standard for the assessment of aortic stenosis. An increase of turbulent energy loss associated with aortic stenosis has been demonstrated in several studies. These losses have to be compensated by increase in the work produced by the left ventricle. Nowadays, echocardiography measurement of the turbulence intensity is not validated for clinical evaluations of aortic stenosis. The aim of this project is to quantify the energy loss associated with turbulent flow in a silicone aortic phantom, using backlight particle tracking velocimetry (PTV) which will be used as gold standard in a subsequent experiment with echocardiography.

## Materials and Methods

Two porcine aortic valves were harvested and inserted in a flow loop that replicates the pulsatile flow of the heart. The flow was recorded with a high-speed camera. The valves were tested under three flow rates (1, 2.5, and 4 l/min). A stiffening of the valves was achieved with formaldehyde and allowed the comparison between valves with native and increased stiffness grade. Forces measurements were performed to assess the stiffness grade of the valves. In addition the pressure in the left ventricle chamber and in the aortic chamber were recorded to evaluate the transvalvular pressure gradient.

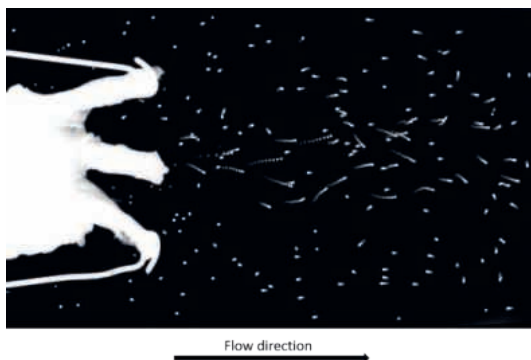


Fig. 1 PTV visualization of the flow in the silicone aortic phantom. The valve is the white shape on the left hand side. Image taken at peak systole. The particles with a long tails indicate high velocity particles.

## Results

The force measurements performed after the stiffening process have demonstrated a significant increase in the stiffness grade of both valves. The transvalvular pressure gradients recorded were systematically higher with stiffer valves (99-123 % higher). Both force and pressure measurements demonstrate the stiffening effect of the formaldehyde on the valves. PTV measurements revealed an explicit increase of the turbulent kinetic energy (TKE) in the aortic phantom after the stiffening process (73.1 % under 1 l/min, and 43 % under 2.5 and 4 l/min).

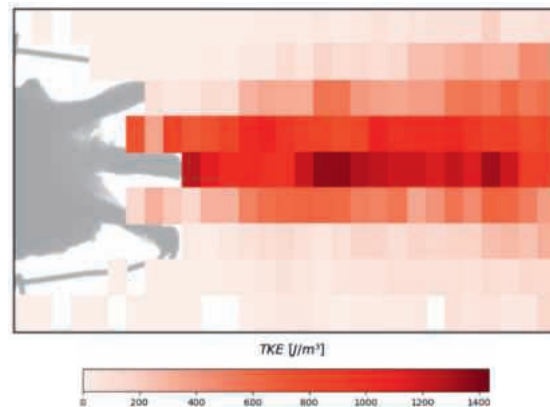


Fig. 2 Turbulent kinetic energy (TKE) at peak systole.

## Discussion

The differences reported above reflect the increased energy loss attributable to turbulence in a model of aortic stenosis. This project has demonstrated the possibility of quantifying an increase of losses attributed to turbulence for porcine valves in vitro with native and increased stiffness grade.

## References

Baumgartner H. et al., "2017 ESC/EACTS guidelines for the management of valvular heart disease", European Heart Journal, vol. 38, no. 36, pp. 2739-2791, 2017

## Acknowledgements

I would like to express my special thanks to Dr. med. Eric Buffle and Prof. Dr. Dominik Obrist for their support throughout the project.

# Orthokeratology - A Biomechanical Model of the Short-Term Refractive Correction

Jeremy Genter

Supervisors: Dr. Miguel Ariza, Prof. Philippe Büchler  
 Institution: University of Bern, ARTORG Center for Biomedical Engineering Research  
 Examiners: Prof. Philippe Büchler, Prof. Dr. Andreas Stahel



## Introduction

Orthokeratology (OrthoK) is a non-invasive and reversible treatment to correct refractive errors, in which a rigid lens is worn overnight. This lens is pressed against the cornea by the eyelid during sleep, inducing a deformation of the corneal epithelium, and consequently, a reduction of the refractive error. After removing the lens in the morning, the original shape of the cornea is slowly recovered. Over time, this mechanical load triggers a mechanobiological response, in which the epithelium is remodeled. The epithelial cells slowly adapt to the desired shape. If the lens is worn often enough, the patient's refractive error is eventually corrected. However, the biomechanical environment of this treatment remains poorly understood. Therefore, this master thesis investigates the hypothesis that the deformation of the epithelium is caused by the redistribution of epithelial fluid within the cornea. Particularly, the short time response of the tissue during the first days of treatment is investigated by using a poroelastic Finite Element (FE) model of the cornea.

## Materials and Methods

A model of the cornea was built using a poroelastic constitutive model (Fig. 1). This model describes the behaviour of a tissue consisting of a porous solid matrix soaked with fluid. The fluid can slowly flow due to the low permeability of the matrix. To identify the material parameters of this model, a population-based evaluation based on 3,500 Monte Carlo simulations was performed to reproduce data available in the literature. To evaluate the calibration of the model, preliminary investigations of personalized simulations have been conducted. The results of patient-specific models were compared to the corresponding experimental data.

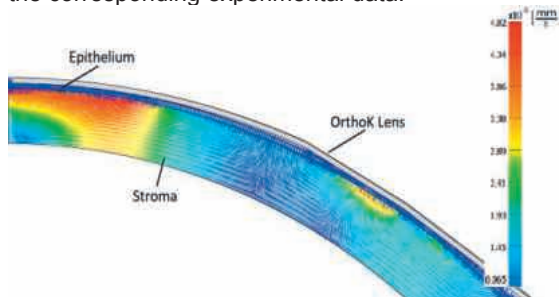


Fig. 1 Fluid flow calculated with a poroelastic constitutive model of the cornea under compression by an OrthoK lens

## Results

The Monte Carlo simulations allowed us to determine the range of material parameters that are able to reproduce the population-based corneal response. The identified parameters are:  $E_{\text{epi}} = 1.39_{-0.5}^{+0.11}$  kPa,

$$k_{\text{epi}} = 3.78_{-1.22}^{+6.26} \cdot 10^{-8} \frac{\text{mm}^4}{\text{Ns}}, k_{\text{stroma}} = 1.17_{-0.46}^{+4.42} \cdot 10^{-3} \frac{\text{mm}^4}{\text{Ns}}.$$

The patient specific FE model was able to reproduce the overall correction observed on the patient (Fig. 2). However, due to the unknown relative position of the lens with respect to the cornea, the simulations were unable to accurately reproduce the local change in the curvature of the cornea.

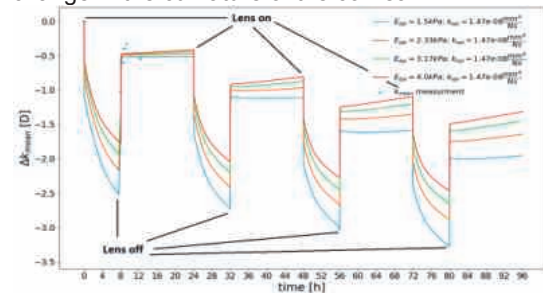


Fig. 2 Initial 4 days of refractive correction achieved during the lens overnight wear (8 h) and daily relaxation (16 h). The evolution of the optical correction is reported for 4 sets of mechanical parameters that able to reproduce short-term clinical data.

## Discussion

The population-based study provided a first assessment of material parameters. However, the lack of extensive experimental data implies that a wide range of parameters, or even several parameter sets, are able to reproduce the refractive correction reported in the literature. With the identified range of parameters, promising patient specific models could be elaborated. Nonetheless, more clinical data is required to sufficiently calibrate and verify the FE model. The inaccuracies of the measurement devices, especially in the periphery of the cornea, does not have a crucial impact on the optics but affects the lens positioning and hence, alters the epithelial deformation. In the future more patient specific data sets will be required to better understand the biomechanical response of the tissue. This proposed model can simulate the short time response of the cornea, which is the first step towards identifying the mechanobiological stimulus responsible for epithelium remodeling.

## References

Alharbi, A. and Swarbrick, H. A. (2003). The Effects of Overnight Orthokeratology Lens Wear on Corneal Thickness. *Investig. Ophthalmol. Vis. Sci.*, 44(6):25182523.

## Acknowledgements

The project was supported by the Vithas Medimar International Hospital, Alicante, Spain. The important contribution of Dr. David Piñero is gratefully acknowledged.

# Development and Evaluation of a Camera Calibration Unit and Procedure for Endoscopes Used in Lateral Skull Base Surgery

Mickael Gerber

Supervisors: Daniel Schneider, Iwan Paolucci  
Institution: University of Bern, ARTORG Center for Biomedical Engineering Research  
Examiners: Prof. Dr. Stefan Weber, Daniel Schneider



## Introduction

Due to geometric scale and proximity of critical anatomical structures, image-guidance for lateral skull base surgery requires a high accuracy (image augmentation error  $< 0.5$  mm) and robust process. It is the main reason why image-guidance technology is not yet applied outside research-related studies.

The goal of this thesis is to develop an endoscope calibration methods and unit, fast ( $< 1$  minute) and easy to use while providing a high accuracy of the final structure overlay. Based on Zhang's camera calibration algorithm, the procedure consists of an acquisition of nine images of a calibration pattern at different distances and angles, imposed by the calibration unit. The latter has been built with 3D printer and a grid of points, visible by the endoscope and the 3D tracking system, is attached to it. In this way, the calibration unit can be tracked, and the endoscope calibrated in the same time. By using the same points for both operations, the manufacturing uncertainties do not influence the accuracy of the calibration. The user is guided through the steps of the calibration by an intuitive graphical user interface.

## Materials and Methods

Two endoscopes are used during this study, one large model designed for endoscopic lateral skull base surgery (diameter: 3 mm, length: 14 cm) and a smaller model, used for inspection of cochlea during robotic cochlear implantation (diameter: 1 mm, length: 6 cm). Both are used with a camera head and tracked in the space via rigidly attached trackers visible by the optical 3D tracking system.

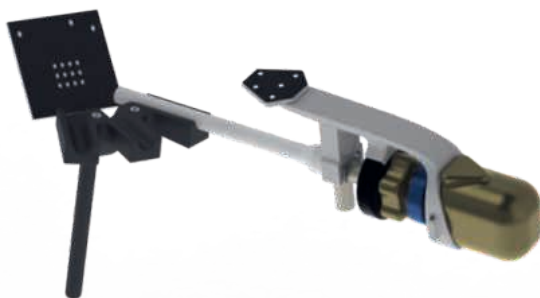


Fig. 1 Endoscope, tracker, lens reinforcement, and calibration unit used during a calibration.

A 3D designed and printed geometrical phantom is created to measure the accuracy of the calibration and a 3D printed human head phantom is used to qualify the usefulness of the calibration in comparable conditions to surgery. Screenshots are stored to measure the distance between objects visible through the endoscope image stream and the superposed virtual models of them.

## Results

An error of  $(0.43 \pm 0.37)$  mm and  $(1.08 \pm 0.62)$  mm is measured with the *large\_3\_mm* and *small\_1\_mm* endoscope respectively.

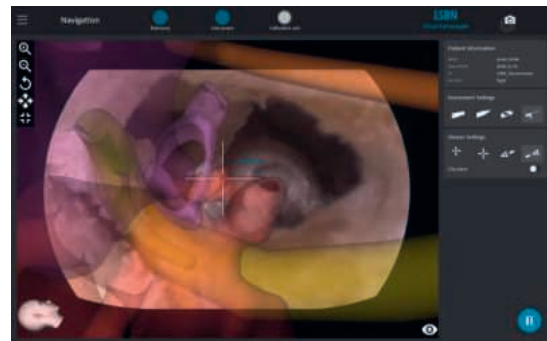


Fig. 2: Overlay result of phantom head through large\_3mm endoscope model.

## Discussion

These results are promising and encourage research in this direction. This thesis lays the foundation for a simple, accurate and robust calibration workflow. A user-friendly graphical interface and calibration unit guiding the user during the calibration process have been successfully implemented. Although the results are not sufficiently accurate for a clinical use, several areas for improvement have been identified.

## References

Schwalbe M. et al., Design and Development of an Endoscope Calibration Method and Unit for Laparoscopic Image Guidance System, 2013.

Garcia J. et al., Calibration of a surgical microscope with automated zoom lenses using an active optical tracker, 2008

## Acknowledgements

The continuous support of Daniel Schneider and Iwan Paolucci is gratefully acknowledged.

# Feasibility Study of Multi-modal Esophageal Measurements for the Monitoring of Preterm Infants

Nishant Gupta



Supervisors: Prof. Dr. Thomas Niederhauser, PD Dr. med. Dr. phil. Andreas Häberlin  
Institutions: Bern University of Applied Sciences, Institute for Human Centered Engineering  
University Hospital Bern (Inselspital), Department of Cardiology  
Examiners: Prof. Dr. Thomas Niederhauser, Dr. med. sc. Kerstin Jost

## Introduction

Monitoring of preterm infants which includes measuring heart rate (HR), respiration rate (RR), oxygen saturation (SpO<sub>2</sub>) and temperature is a vital function performed by the Neonatal Intensive Care Units (NICU). However, current systems use skin-attached electrodes and sensors which damage the infant's skin and are prone to be inaccurate. Multi-function esophageal catheters which combine the monitoring function with enteral feeding is a promising solution to replace surface sensors. However, currently available catheters lack the variety of sensing modalities needed and their manual construction using wires and passive sensors making further additions difficult. The aim of this study is to develop a novel approach of manufacturing catheter having multiple sensing modalities and to develop data fusion algorithms that can extract relevant parameters from the multi-channel data with increased accuracy and robustness.

## Materials and Methods



Fig. 1 Catheter circuit layout containing active transducers and signal conditioning. (Top: Unfolded, Bottom: Folded)

LCP based flexible circuit together with miniature surface mount components was used to develop a catheter layout which can measure bio-potentials, pressure, photo-plethysmograph (PPG) and temperature (Fig. 1). Alternate circuits were devised where standard methods would require too large components. Interfacing multiple modalities required a novel multiplexing system which uses only two connections to select between multiple sensor nodes. Circuit validation was performed using test-PCBs having same circuit schematics but larger counterparts of the sensors and transducers. For data fusion, an existing multi-channel esophageal ECG data from preterm infants was used to extract respiration rate from baseline wander. Model based approach using Kalman algorithm was developed to combine data from all channels. The results were compared against RR obtained using chest impedance (CI) by a standard NICU. Median (interquartile range) deviation in units breaths per

minute (bpm) from a reference RR created using inspiration and expiration peaks labeled by trained physicians was used to compare accuracy.

## Results

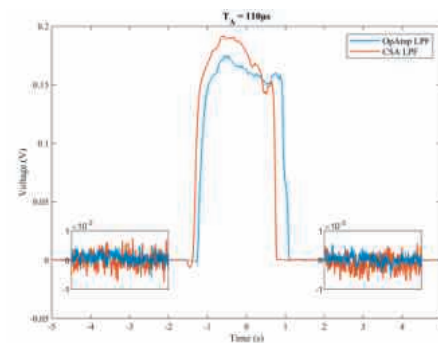


Fig. 2 Voltage output from two different pressure measurement circuits under application of 100mmHg pressure pulse. (Inset: zoomed y axis for noise comparison)

Measurements of ECG, pressure (Fig. 2) and PPG obtained using the test PCBs were found to have good signal quality. Multiplexing system also worked while allowing adequate data rate. RR extracted using Kalman algorithm were found to have lower median deviation (0.34 (-2.75 to 2.65) bpm) from the reference compared to CI RR (-6.96 (-10.50 to -4.14) bpm).

## Discussion

Proposed catheter manufacturing method and circuit layout offers numerous advantages with regards to increased monitoring capability, improved signal quality and simpler manufacturability compared to existing multi-function catheters. The current design, however, can be improved using mechanical optimization via 3d modeling. Future advancements in sensor technology and flexible electronics would further increase flexibility and reduce size.

## Acknowledgements

I would like to thank my supervisors Prof. Dr. Thomas Niederhauser and PD Dr. med. Dr. phil. Andreas Häberlin for their constant motivation and scientific guidance throughout this study. I would also like to thank my colleagues at HuCE-microlab for their practical help in designing the catheter.

# Contactless Detection of Gait and Gait Abnormalities

Nathan Gyger



Supervisors: MSc Angela Botros, MSc Narayan Schütz  
Institution: University of Bern, ARTORG Center for Biomedical Engineering Research  
Examiners: Prof. Dr. Tobias Nef, Prof. Dr. med. Paul Krack

## Introduction

In Switzerland, more than 15'000 people suffer from Parkinson's disease (PD). Gait disturbances are a classical symptom of the disease which strongly impact mobility in affected people. Gait disturbances can be alleviated using a drug-based medical treatment. However, the effectiveness of the treatment fluctuates throughout the day. Therefore, to quantify gait parameters and to evaluate symptom fluctuations at home, a compact and contactless gait tracking system based on 2D scanning rangefinders installed in a home-like environment is proposed.

## Materials and Methods

Several scanning rangefinders are fixated close to the walls 25 cm above floor level. They generate 2D point clouds which are processed to identify leg positions. Background subtraction and clustering methods are used in the identification process, whereas particle filtering deals with potential occlusions. Leg velocity profiles are then computed from the leg positions and used to assess gait parameters.

A study with 27 healthy young controls asked to walk according to both controlled and uncontrolled gait patterns was performed. To evaluate the results, the proposed system was compared to a gold-standard gait tracking system (GAITRite®). All measurements were performed at the Neurotec Loft (NL), which is a home-like experimental setup within the sitem-insel building in Bern, Switzerland.

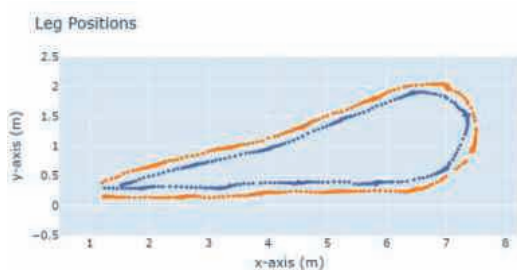


Fig. 1 Identified left leg (blue) and right leg (yellow) positions during a non-straight walk.

## Results

The scanning rangefinder system could successfully extract leg velocity profiles and compute relevant gait parameters. The accuracy achieved by the scanning

rangefinder system in the validation study showed no significant difference with that of the gold-standard system for most of the investigated gait parameters. The smallest mean deviation from the reference value is of -0.28% (std 2.28%) for stride length and the largest mean deviation is of +8.24% (std 5.36%) for cadence.

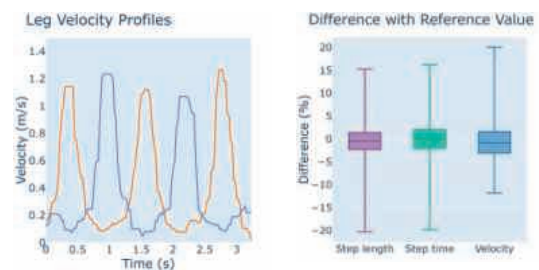


Fig. 2 The right part depicts the velocity profiles of the right leg (blue) and the left leg (yellow). The left part summarizes the difference in percentages between the scanning rangefinder system and the reference system for three selected gait parameters.

## Discussion

The developed system is a promising solution for long-term tracking of gait parameters at home in PD patients. Its contactless and compact nature makes it less invasive than other existing systems. Moreover, the type of acquired data (2D point clouds) preserves the intimacy of the patient. For these reasons, the system is likely to have a high acceptance in patients. The validity of the system in people with neurological disorder will be evaluated in a future clinical trial and its potential usability for fall-risk assessment in the elderly will be studied.

## References

L. M. de Lau and M. M. Breteler, "Epidemiology of Parkinson's disease," *Lancet Neurol.*, vol. 5, no. 6, pp. 525–535, Jun. 2006, doi: 10.1016/S1474-4422(06)70471-9..

## Acknowledgements

I would like to thank all the members of the Gerontology and Rehabilitation group for their precious inputs and continuous support throughout this thesis. Special thanks also go to the neurology group of the insel-spital for providing the reference gait tracking system for the validation process.

# Robot Virtual Deletion: Using immersive Virtual Reality to Hide the Robot During a Robot-assisted Motor Task

Mirjam Jordi



Supervisors: MSc Nicolas Wenk, Prof. Dr. Laura Marchal-Crespo  
Institution: University of Bern ARTORG Center for Biomedical Engineering Research  
Examiners: Prof. Dr. Laura Marchal-Crespo, MSc Nicolas Wenk

## Introduction

To restore independence and to improve functional recovery in stroke patients, robotic devices are nowadays often employed because they can provide high-dose and high-intensity training. For a successful rehabilitation intervention, patients' motivation plays an important role. However, the patient's motivation during robotic-assisted rehabilitation is generally low. To overcome this limitation, virtual reality (VR) has been proposed as an add-on to robotic rehabilitation. When immersive VR (IVR) and robot-assisted rehabilitation are combined, the robot is normally not shown in VR. This could create a sensory conflict between feeling forces but not seeing their source. On the other hand, not rendering the robot in VR could increase the participant's motivation, since they might believe they are doing the task without any external help. This project aimed to investigate if the virtual deletion of the robot during a robot-assisted motor task in IVR has an impact on the users' subjective experience.

## Materials and Methods

A blinded within-subject pilot study with sixteen healthy participants was designed, developed, and carried out. During the experiment, the participants were asked to perform a path-following task in IVR while being attached to a robot (Fig.1). Two control modes were evaluated. One in which the robot did not exert any force (i.e., transparent mode) and one in which an assisting force was applied when the participants' hand left the path (i.e., path control). In each control mode, the participants performed the task once with a visible robot and once with an invisible robot.

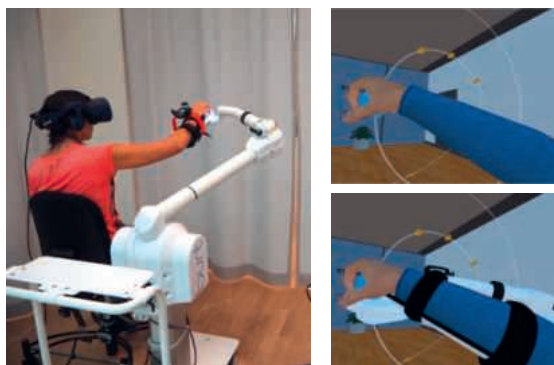


Fig 1 Left: a participant performing the task. Right: Participants' view during the task. Above with an invisible robot and below with a visible robot.

After each performed task, the participants had to fill in a questionnaire about their motivation, their feeling of presence, and their feeling of body ownership and agency.

## Results

No interaction effect was found between the two controller modes and the visibility of the robot. However, according to the answers from the subscales of the motivation questionnaire, participants put significantly more effort into the task when they saw the robot in IVR than when they did not see the robot ( $p = 0.002$ ). Furthermore, participants tend to trust the robot more when they did see it in VR (i.e., higher relatedness,  $p = 0.059$ ). No differences were found between doing the task with an invisible or visible robot in the sense of presence, body ownership, and agency. Interestingly, we found that training with the path-controller increased participants' motivation, reduced the sense of presence, and reduced body ownership compared to training without robotic assistance.

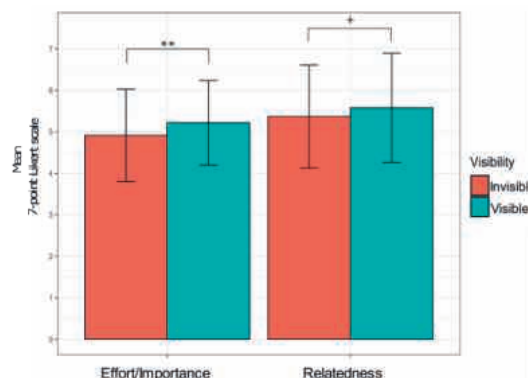


Fig 2 Mean values for the motivation subscales Effort/Importance and Relatedness.

## Discussion

The expected sensory conflict of feeling a robot but not seeing it did not harm participants' experience. Contrary to our expectations, we observed an increase in some motivation subscales, namely Effort/importance, and Relatedness when the robot was visible.

## Acknowledgments

This work would not have been possible without the great support from the Motor Learning and Neurorehabilitation Laboratory. Thanks to all the participants who took part in the study.

# Creating Radioactive Patches for Skin Cancer Therapy Based on 3D Printing Technology

Prajit Kadavil



Supervisors: Prof. Dr. J. Burger, Dr. A. Boese  
Institutions: University of Bern, Sitem Center for Translational Medicine and Biomedical Entrepreneurship  
OVGU – University of Magdeburg, INKA  
Examiners: Prof. Dr. J. Burger, Dr. L. Galéa

## Introduction

The standard procedure for non-melanoma skin cancer (NMSC) is surgery. Non-surgical procedures, radiation therapy, have proven to be effective treatment. In radiation therapy gamma- or x-rays are often used. These type of radiation have the disadvantage that they penetrate deep into the bone, which is a radiation sensitive structure. A better alternative would be an application with beta emitters, as these particles have a lower penetration depth. Furthermore the shielding is easier than with gamma radiation or x-ray [1]. Several concepts for creating radioactive patches with beta emitting radioisotopes for use on skin cancer have been developed at the chair of INKA, University of Magdeburg. There is, despite this, no workflow that radioactive patches can be used in a clinic. The goal of this thesis was to develop requirements for the application for tumor specific patches and to focus on the implementation in a clinical department.

## Materials and Methods

A workflow for radioactive patches was proposed for applications with beta emitter sources for NMSC. Two concepts were considered patches with liquid radioactive source and solid ones. Literature review has been done, and companies contacted that can supply these sources. The focus was on suitable concepts with beta emitters. As proof of concept, a method using pipetting was attempted to keep a non-radioactive liquid mixture of water, ink and hydrochloric acid in place, which was distributed on adhesive tape with superabsorbents (Schneiders Profiechemie GmbH & Co. KG (Ilfeld, Germany)).

## Results

Droplets of the ink solution could match the shape of the tumor. A volume of 0.1 ml would cover a surface with a diameter in average of 18.2 mm. A process map for radioactive patches was proposed that was adapted from ocular brachytherapy [2] (figure 1): Using image data of the tumor, the required activity of the radioisotope is determined. During preparation, a dosimetrist or radio chemist prepares the patch. In the case of enclosed radionuclides, a radiotherapist would perform this application on patients; in the case of open radionuclides, the nuclear physician would be needed. With a solid radioisotope compared to the liquid one, no preparation of the radioactive material would be needed, which would require fewer regulations and restrictions for handling. Suitable radioisotopes for a patch application, which can be purchased in

Europe, would be: Rhenium-188, Yttrium-90, Ruthenium-106. Y-90, which costs up to 21 Euro/mCi (PerkinElmer Inc., Massachusetts, U.S.). or a Re-188 generator which could produce 1 Curie per week, and costs around 3600 Euro (Oak Ridge National Laboratory, Tennessee, U.S.). The company Eckert&Ziegler AG, Berlin, Germany is coating their eye applicator with Ru-106. Prices start at 14'000 Euro.

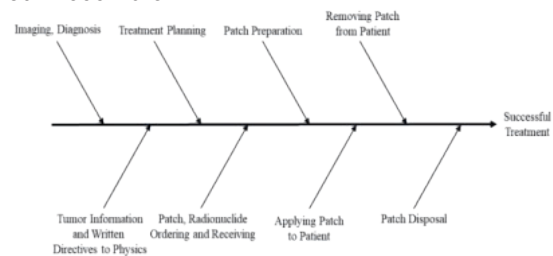


Fig. 1 Proposed process map for using radioactive patches in clinics (adapted from [2])

## Discussion

Pipetting requires training for handling the radionuclides. An adhesive tape is flexible and can be shielded from radiation by additional protective layers. Even when considering a radionuclide solution, tumor sizes smaller than 18mm in diameter could not use all of the 0.1mL solution available from the supplier, resulting in a loss of radioactivity for treatment. Furthermore, the distribution of the radioactivity in the solution is not known. To ensure that the radioactive solution on a medical tape with a super absorber is compatible, a test would have to be examined. Instead of using liquid solution, a solid form of radioisotope can be applied in an applicator. However, the solid form of radioisotope will be stiffer and limited in diameter.

## References

- [1] A. Pashazadeh, A. Boese, and M. Friebe. Radiation therapy techniques in the treatment of skin cancer: an overview of the current status and outlook. *Journal of Dermatological Treatment*, 30(8):831-839, 2019. PMID: 30703334.
- [2] Y. C. Lee, Y. Kim, J. W.-Y. Huynh, and R. J. Hamilton, "Failure modes and effects analysis for ocular brachytherapy," *Brachytherapy*, vol. 16, no. 6, pp. 1265-1279, 2017.

## Acknowledgements

I would like to acknowledge Prof. Dr. Burger, Prof. Dr. Friebe and Dr. Galéa who accepted to supervise my thesis. Many thanks to A. Pashazadeh for guiding me to my goal.

# Feasibility of Transesophageal Phrenic Nerve Stimulation

Elisa Maria Kaufmann



Supervisor: MSc Samuel Kreuzer  
Institution: Bern University of Applied Sciences, Institute for Human Centered Engineering HuCE-microLab  
Examiners: Prof. Dr. Thomas Niederhauser, Dr. Dr. med. Andreas Häberlin

## Introduction

Natural inspiration leads to a negative intrapleural pressure, resulting in a pressure gradient between the atmosphere and the pulmonary alveoli, from which inhalation results. During mechanical ventilation (MV), this pressure gradient is created by a positive pressure from a ventilation source. The main respiratory muscle, the diaphragm, remains passive. Only six hours of MV can lead to muscular atrophy due to inactivity of the diaphragm. If the phrenic nerve and diaphragm are intact, electrical stimulation of the N. phrenicus can induce a contraction of the diaphragm, whereby inhalation occurs. The lungs are again under negative pressure, thus making breathing more natural. This thesis proposes a new, non-invasive approach, where the phrenic nerve is activated by electrical stimulation impulses from the esophagus.

## Materials and Methods

The optimal stimulation position was defined, based on an anatomy study. In order to represent the reactions of electrical stimulation, in vitro experiments were used to investigate favorable stimulation parameters. The electrode configuration and size were also considered, with focus on the alignment of the electrode segments. This allowed the comparison of segmented and conventional omnidirectional stimulation electrodes. A suitable measurement setup was established according to the defined stimulation protocol, through which the activation of the phrenic nerve and the diaphragm can be recorded.

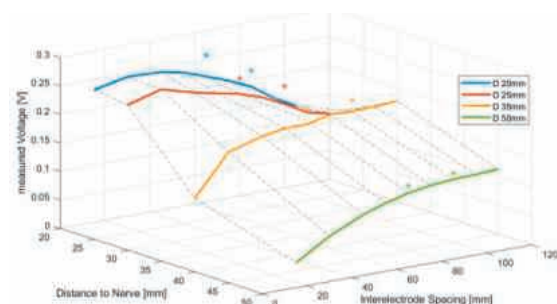


Fig. 1 In the in-vitro measurements various distances to the target structure, spacings and electrode sizes were evaluated. The measurement points marked as stars show the yield of the segmented, nerve-aligned electrodes.

## Results

The localization of the optimal stimulation positions was done by means of dissection, MRI and

ultrasound examinations. The most suitable interelectrode spacings and stimulation amplitudes

were determined in saline solutions at the expected distance between N.phrenicus and esophagus and were evaluated using Matlab R2019b (Fig1). Using segmented electrodes aligned to the nerve, a voltage gain of up to 12.5 % could be achieved. In addition, co-stimulation of surrounding tissue at 120° behind the stimulation electrode was reduced by more than 30%

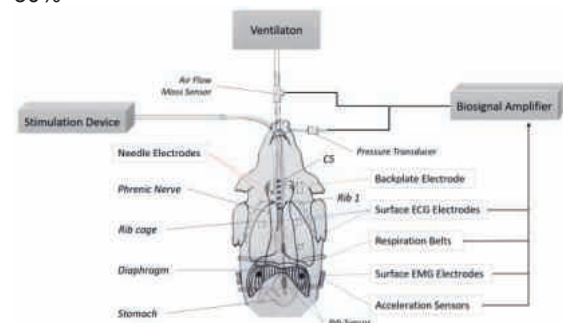


Fig. 2 The resulting setup for an upcoming animal trial to verify the feasibility of transesophageal stimulation. A comprehensive measurement setup is available to record a successful activation of the phrenic nerve or diaphragm.

## Discussion

The anatomical studies of humans and pigs resulted in the same conclusion, which validates the use of a pig as translational research model in this application. The choice of electrode size and electrode segments allows a selective activation of the phrenic nerve and reduces the undesired co-stimulation of nontargeted nerves. The informative value and reliability of the in vitro measurements are confirmed by the high reproducibility of the ex vivo experiments. The setup (Fig. 2) and protocol for the upcoming animal study are the result of the combined outcomes of the anatomy study and the experimental studies, which will allow to verify the feasibility of transesophageal stimulation. The more natural inspiration will result in faster patient recovery and reduce the duration of treatment, which generally leads to lower health care costs and improved quality of life.

## References

S. C. Reynolds et al., "Mitigation of Ventilator-induced Diaphragm Atrophy by Transvenous Phrenic Nerve Stimulation," Am J Respir Crit Care Med, vol. 195, no. 3, pp. 339–348, Aug. 2016.

# Feasibility Study of a Rechargeable Implantable Continuous Cardiac Monitor

Sven Krause



Supervisors: Prof. Dr. Thomas Niederhauser, Samuel Kreuzer  
Institution: Bern University of Applied Sciences, Institute for Human Centered Engineering HuCE  
Examiners: PD. Dr. Thomas Niederhauser, PD. Dr. med. Dr. phil. Andreas Häberlin

## Introduction

Heart rhythm disorders, i.e. arrhythmias are pathologies of the electrical system of the heart leading to irregular heartbeats that are either too fast or too slow. The increasing prevalence of arrhythmias is attributed to the ageing population and rising number of chronic heart diseases. Conventional Holter monitor or implantable loop recorders (ILR) measuring the electrocardiogram (ECG) can be used to diagnose infrequent arrhythmias that lead to recurrent palpitations, syncope or cryptogenic strokes in the patient.

Implantable loop recorders are implanted subcutaneously and are event recorders that record the ECG of the heart and only save information of an abnormal and irregular cardiac activity. This limits the accuracy to detect potentially asymptomatic arrhythmia such as paroxysmal atrial fibrillation.

To overcome these limitations, a feasibility study on a rechargeable implantable continuous cardiac monitor (ICCM) allowing recordings of two lead ECG for months to years with the capability to read data transcutaneously and charge the battery wirelessly for continuous and uninterrupted measurements has been made.

## Materials and Methods

A development and transmitter board mimicking the electrical functionality of the implant and the extracorporeal charger, respectively. Three aspects of the implant were studied in detail: the comparison of two different analog front ends for ECG measurements, the characterization of wireless power transfer through different coil designs and the optimization of the power consumption.

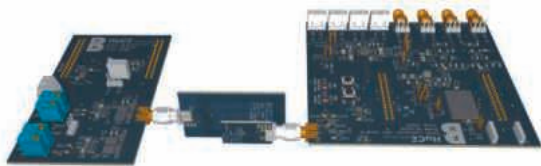


Fig. 1 Development board and transmitter board used to determine the feasibility of a rechargeable implantable continuous cardiac monitor.

The setup was made in a way that all the main functional blocks are separated and easily accessible. The coils are separated from the boards to allow fast and versatile measurements. Wireless power transfer is done using two inductive coupled

coils resonating at 6.78 MHz and Data transfer is achieved using Bluetooth Low Energy.

## Results

The wireless power transfer system showed that, with optimal coils parameters, it is possible to recharge a 50mAh battery over 30 mm without the need of perfect coil alignment. The two analog front ends didn't show noticeable differences in noise level compared to each other but differed in power consumption.

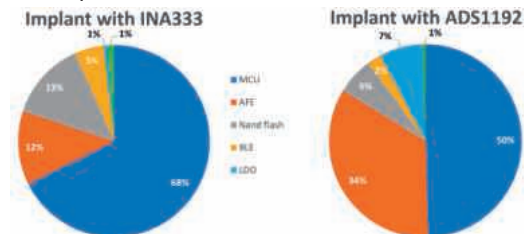


Fig. 2 Power consumption of the implant using an INA333 as an AFE (left) and the ADS1192 as an AFE (Right)

The analog front end with the lowest power consumption has been adopted for the rest of the study. The consumption of the entire system was measured to be 1.47 mA.

## Discussion

A fully functional wirelessly rechargeable implantable continuous cardiac monitor was developed. The device can sample two leads ECG at a sampling rate of 250 Hz continuously. It can acquire data for around 1.4 days before the battery has to be recharged. Further research on lowering power consumption should be conducted. Using for example an application-specific integrated circuit (ASIC) rather than a general-purpose chip could lower the overall power consumption and thus extend the time between charging cycles. Next steps of this feasibility study should then focus on miniaturizing the working circuit on a flexible PCB made out of liquid crystal polymer (LCP) and test the implant in an animal trial to fully prove that the concept works.

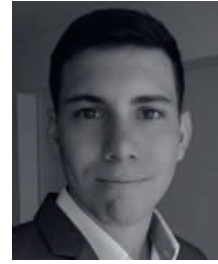
## Acknowledgements

I would like to thank my two supervisors, Prof. Dr. Thomas Niederhauser and Samuel Kreuzer, for their expertise and knowledge. Also, I would like to thank all my colleagues from the HuCE-microLab for their help and support during all my thesis.

# CFD-Based Characterization of Thermobonded LCP Catheters

Oliver R. Lammer

Supervisors: Prof. Dr. Thomas Niederhauser, Prof. Dr. André Lisibach  
Institution: Bern University of Applied Sciences, Institute for Human Centered Engineering HuCE-microLab  
Examiners: Prof. Dr. Thomas Niederhauser, Prof. Dr. Andreas Stahel



## Introduction

Nowadays, surgical operations are increasingly using minimally invasive procedures with sophisticated medical tools such as catheters. The laborious manufacturing of such catheters presents a need for the development of an automatic production via a thermobonding process. During the process, a liquid crystal polymer (LCP)-based flexible printed circuit board (FPCB) is laminated to a thermoplastic elastomer (TPE) catheter tube. To improve the surface adhesion, microholes were incorporated in the FPCB design. The filling quality of the microholes is an essential factor for a strong delamination resistance when the catheter is pulled and bent. To reliably predict the microhole filling, the thermobonding process is implemented into 2D Finite Element Analysis (FEA) models, using COMSOL Multiphysics® 5.5, and validated with experimental trials.

## Materials and Methods

The thermobonding process for a 3 lumen catheter was decomposed into 3 models, based on the TPE material states. In the first mechanical step of the process, the model is preformed by a compressing ring form. To evaluate the amplitude of the compression, experimental tests were conducted. In the second mechanical model, the heated TPE thermally expands until reaching its melting temperature.

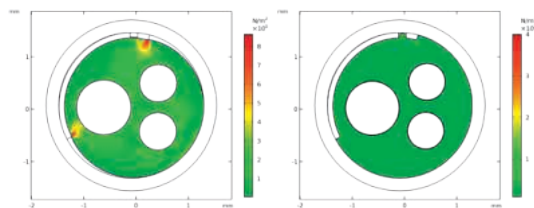


Fig. 1 On the left, the preformed catheter model and on the right, thermally expanded TPE at melting temperature.

The resulting deformed geometry is then used as the initial model for the computational fluid dynamic (CFD) problem. The level set method was used to trace the fluid interface when the microhole is filled. Temperature dependent viscosity was considered and the thermal expansion of the liquid TPE could be reliably implemented based on a heat transfer study.

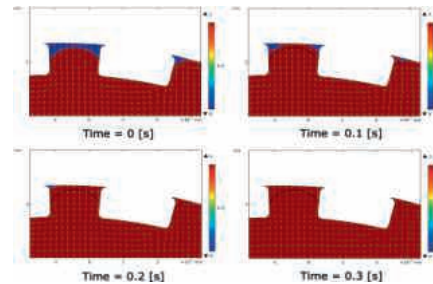


Fig. 2 Filling of the microhole at different time steps. The remaining solid components were defined as fixed boundaries.

## Results

The combined models were able to correctly reproduce the filling process of the microholes. The structural mechanics, heat transfer and CFD models demonstrated efficiency and numerical stability. The thermobonding models were applied on potential dimension issues with production components and reliable outcomes were determined, showing dimension and time consistencies.



Fig. 3 Microscope pictures of the microholes after thermobonding. On the left, a delaminated FPCB and on the right, a laminated FPCB.

## Discussion

COMSOL was successfully used to model the thermobonding process and the results showed close agreement with experimental data. The simulation results provide valuable insight on how the production parameters affect the final catheter. By manipulating parameters such as the microhole dimensions and material properties, the simulations can be used to optimize the production process, ultimately saving time and valuable resources.

## References

[1] G. Kuert, M. Jacomet, and T. Niederhauser, "Efficient thermobonding process forming a polyurethane based diagnostic catheter with liquid crystal polymer", presented at the 2019 41st Annual International Conference of the IEEE Engineering in Medicine and Biology Society (EMBC), Jul. 2019.

# Budget Annotation for Supervised Machine Learning Methods

Britton B. Marlatt



Supervisors: Dr. Pablo Márquez-Neila, Prof. Dr. Raphael Sznitman  
Institution: University of Bern, ARTORG Center for Biomedical Engineering Research  
Examiners: Dr. Pablo Márquez-Neila, Prof. Dr. Raphael Sznitman

## Introduction

Annotations are fundamental to supervised machine learning, as they offer meaningful examples which inform the model and provide a learning basis for future interpretation. Unfortunately, modern machine learning techniques rely on large amounts of labeled data in order to train and refine internal parameters. This is particularly problematic in the medical domain, given the cost, time and noise associated with annotations from medical experts. However, as medical data continues to grow, large unlabeled datasets, or 'data lakes,' are abundant. A recent method developed in the AIMI Lab, ARTORG, embeds raw image data into a smart latent space. This thesis aims to apply smart sampling methods on the latent space from a data lake of retinal OCT B-scans to select a subset of images from the training set. In turn, the annotated data will train a deep learning network under a budget constraint. The model performance for each sampling technique is compared to random selection as a baseline. The goal is to learn a good classifier on a given budget.

## Materials and Methods

Three training experiments were conducted. The first experiment investigates the relationship between training budget constraints and deep learning model performance. The second experiment explores the effects of smart sampling procedures with a budget constraint on the model performance compared to random selection as a baseline. And the third experiment tests how the best sampling method performs in the presence of data imbalance.

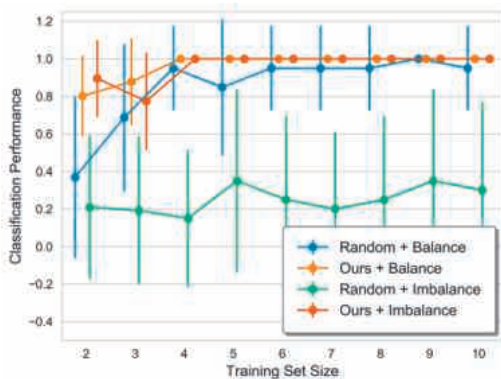


Fig. 1 Our method's performance (AUC) versus random selection given a balanced and imbalanced dataset (MNIST-CIFAR).

The selection methods developed in this thesis employed machine learning techniques such as  $k$ -means and  $k$ -medoids clustering, Gaussian mixture models, Akaike information criterion, support vector machines, principal component analysis and  $t$ -distributed stochastic neighbor embedding.

## Results

The best-performing selection strategy used a  $k$ -means stratified random sampling approach that reorganizes the latent space into an optimal number of strata, which are then proportionally randomly sampled. On the retinal OCT dataset its classification performance exceeds random selection averaged over 10 trials. It also outperforms random selection in the imbalanced experiment conducted on an MNIST-CIFAR combination dataset.

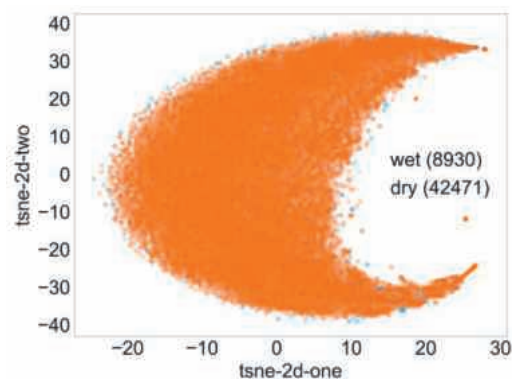


Fig. 2 2D  $t$ -SNE representation of the homogeneous distribution of label classes in the 32-dimensional retinal OCT latent space.

## Discussion

The results indicate our budget-constrained sampling method is better than pure random sampling. Further investigation into the latent space found that the latent features fail to recognize retinal fluid in its 32 latent features. Further investigation into the feature dimension in the latent space is required.

## Acknowledgements

This thesis was fulfilled in the Artificial Intelligence in Medical Imaging Laboratory. The important contribution of Dr. Márquez-Neila for the data materials, trained latent spaces, and deep learning network architecture is gratefully acknowledged.

# A Right Heart Mock Circulation Setup Allowing for Enhanced Cardiovascular Imaging – A Simulation Study

Tamara Stefanie Melle



Supervisors: PD Dr. med. Dr. phil. Andreas Häberlin, Dr. Adrian Zurbuchen  
Institutions: University Hospital Bern (Inselspital), Department of Cardiology  
sitem Center for Translational Medicine and Biomedical Entrepreneurship  
Examiners: PD Dr. med. Dr. phil. Andreas Häberlin, Dr. Adrian Zurbuchen

## Introduction

Before a new cardiovascular medical device can be used for lifesaving interventions, it first has to undergo multiple tests in vitro. A human mock circulation loop makes these tests possible. Most of the already existing mock circulation loops are designed for the left heart side only. Loops for the right heart side suffer from limitations. Thus, the need to find a setup to simulate physiological pressures and flows for the right heart side was identified. A modular construction concept should allow the usage of the setup for various applications. The development of a simulation, predicting the flow loop metrics for different scenarios, was defined as the key goal for this thesis.

## Materials and Methods

A simulation approach with electric and hydraulic simulations, done in SIMULINK (The MathWorks Inc., USA), was chosen to define metrics of a physical setup. Physiological reference values were translated to the simulations, based on the electric-hydraulic analogy. Most of the necessary metrics for a first prototype were provided by the hydraulic simulation. A validation setup was built subsequently. The loop was driven by a ViVITro SuperPump (ViVITro Labs Inc, Victoria, BC, Canada) and pressures in the compliance chambers were measured with pressure sensors (MLT0670, ADInstruments Ltd., United Kingdom).

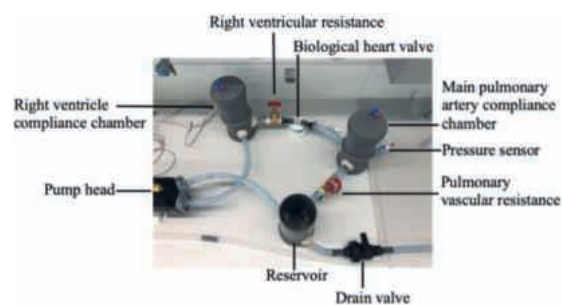


Fig. 1 Validation setup from a bird's-eye view.

## Results

Pressure and flow curves, close to their physiological reference could be achieved with the hydraulic simulation of the validation setup. In real-life, the measured pressure values for the prototype reached a much bigger amplitude of the pressure curves in both compliance chambers.

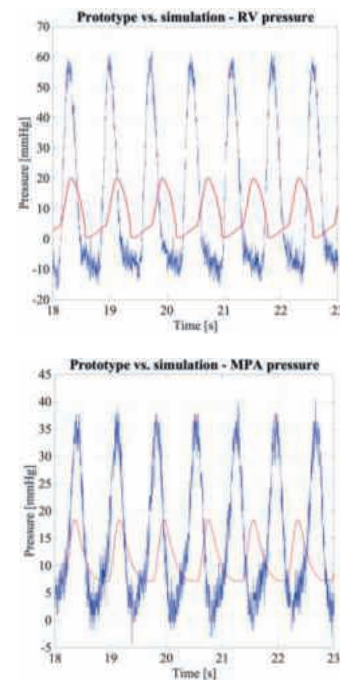


Figure 2 Comparison of the simulated pressure curves with the measurements of the prototype for the right ventricle (RV) and the main pulmonary artery (MPA).

## Discussion

The pressure curves of the prototype showed the desired periodic behavior but were not completely satisfying regarding to their maximal and minimal values. The pressure differences between the simulation and the setup indicated that the air chambers of the compliance chambers were too small. Due to this, the connection between the components of the simulation and the real-world will need to be improved.

## Acknowledgements

I would like to express my special thanks to my two supervisors, PD Dr. med. Dr. phil. Andreas Häberlin and Dr. Adrian Zurbuchen, who supported me during all these months of this thesis with their expertise. Also, I would like to thank all my colleagues from the Cardiac Technology and Implantable Device group.

# Focused Cross-Modality Hip Joint Segmentation For FAI Diagnosis

Cédric Moser



Supervisors: Dr. Nicolas Gerber, Dr. Guodong Zeng  
Institution: University of Bern, sitem Center for Translational Medicine and Biomedical Entrepreneurship  
Examiners: Dr. Nicolas Gerber, Dr. Kate Gerber

## Introduction

Osteoarthritis (OA) is a degenerative joint deformity that causes pain and is seen as one of the main causes of physical disability. Femoroacetabular impingement (FAI) is a condition in the hip joint that has recently been recognized as a key risk factor for the development of early cartilage damage and is a possible precursor of hip OA. In order to diagnose FAI as well as plan and simulate the treatment, a 3D segmentation of the hip joint based on MR images is needed. Recently, deep learning based methods have shown an excellent segmentation performance. However, these methods suffer from the domain shift problem, where the segmentation performance drops significantly when a domain gap between source and target domain exist. Domain gaps include multiple differences such as various image protocols or modalities. However, manually labeling medical images is usually prohibitively expensive or impractical, to retrain a new supervised model. This thesis aimed to use unsupervised learning approaches to eliminate the need for additional labeled data. Specifically, we trained a deep learning based cross-modality hip joint segmentation model to segment MR images based on the unlabeled images and the corresponding labelled CT images illustrated in figure 1.

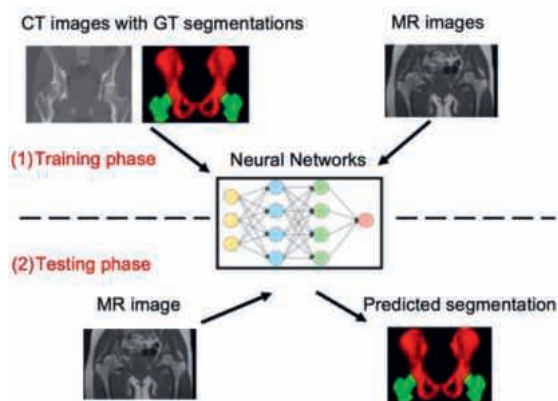


Figure 1 Deep learning based cross-modality hip joint segmentation model.

## Materials and Methods

We developed a segmentation pipeline based on an image adaption step which is illustrated in figure 2. First, the MR image is translated (1) via the image-to-image adaption technique CycleGAN, to a

synthetic CT image. Then the synthetic CT image is segmented with our supervised segmenter (2), which has been trained on the labeled CT data.

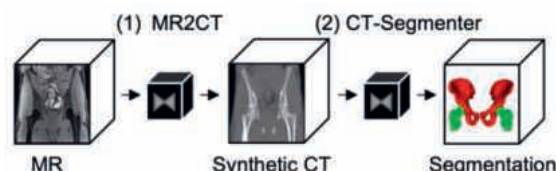


Figure 2 Workflow of the unsupervised cross-modality segmentation for the hip joint MR images.

To further reduce the domain gap the field of view in the training data from the two domains was cropped prior to application of the segmentation pipeline.

The accuracy of the proposed segmentation pipeline relative to the state of the art application of the CT trained segmenter to MRI, was evaluated by comparing automatic segmentation results to ground truth manual segmentations using the dice overlap coefficient (DOC).

## Results

Compared to the original CT trained segmenter applied to directly to MR image data without domain adaption, our method improved the DOC from 0.3% to 82.8% for the pelvis and from 0.0% to 85.9% for the femur. The qualitative inspection of the results disclosed that larger segmentation errors were mainly found when the image translation quality was low in the image translation step from MR to synthetic CT.

## Discussion

With the improved results compared to the current state of art we demonstrated the effectiveness of our method. Depending on the required accuracy, manual corrections to the segmentation may be required. However, our proposed method removes the need for additional time-consuming and costly annotation on the target domain.

## Acknowledgements

We would like to thank our clinical partners Dr. med. Till Lerch and Dr. med. Florian Schmaranzer for providing the training data and for providing medical expertise during this thesis.

# Real-time Observation and Feedback System for 3D-Bioprinting Dispensing Technologies

Thiago H. Pincinato



Supervisor: Prof. Dr. Patrik Arnold  
Institution: Bern University of Applied Sciences, Institute for Human Centered Engineering, HuCE-optoLab  
Examiners: Prof. Dr. Partik Arnold, MSc. Dominic Ernst

## Introduction

Three-dimensional bioprinting is a growing field that provides a revolutionary platform for the development of the medical sciences. It has been significantly used in numerous research from various academic disciplines [1,2]. Despite the potential of this emerging technology, the lack of a real-time observation system makes it difficult to assure the correctness of the three-dimensional printed structure. Depending on the bioink properties and process parameters, the shape accuracy may deviate from the designed models. Most of the current toolpath planning approaches for bioprinting do not consider the changes in shape of soft bioink [1]. This thesis works towards developing a system capable of observing the dispensing process of three-dimensional bioprinting technologies in real-time.

## Materials and Methods

Four miniaturized multi-view prototypes were designed and developed. Those prototypes were used to perform experiments with different cameras, their placement and the impact of lighting conditions on the recorded data. Additionally, images acquired by the most suitable prototype were submitted to a sequence of image processing techniques. The applied techniques can be divided in two main groups, segmentation and fiber reconstruction. For the segmentation, a Canny edge detection, super pixel and a Ransac mathematical fit model algorithms were utilized. Regarding the reconstruction, images from three different cameras were combined to generate a three-dimensional representation of the fiber.

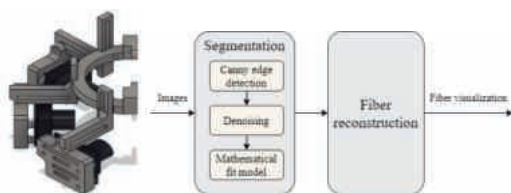


Fig. 1 Overview of the developed observation system for 3D-bioprinting dispensing technologies.

The prototypes were compared in respect to their usability and capability of capturing the dispensing fiber. For the image processing, the performance was statistically measured via sensitivity, specificity and execution time.

## Results

The system achieved sensitivity values between 73,24% and 90,48%, and specificity values between 99,92% and 99,99%. Both values are strongly influenced by the canny edge parameters. The time necessary for processing a single image was equivalent to 675 milliseconds.

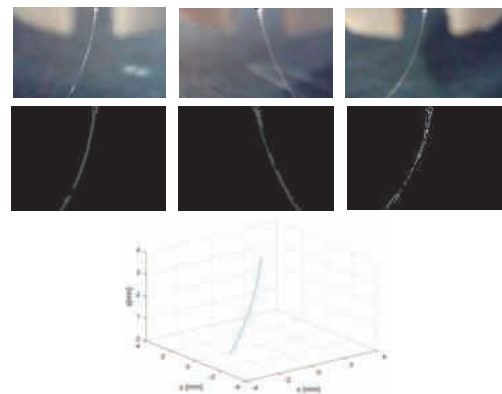


Fig. 2 Example of acquired images (top row), segmentation (middle row) and fiber reconstruction (bottom).

## Discussion

This thesis confirms that, despite the small thickness of the fiber, it is possible to use commercial cameras for the observation of 3D bioprinting dispensing technologies. As expected, the quality of the acquired images plays a major role on the results of the image processing. In situations where the entire fiber was captured, the fiber segmentation was effective and robust against noise. The fiber reconstruction technique provides a clear visualization of the fiber shape within some milliseconds. Nevertheless, the required execution time for the chosen segmentation techniques is an obstacle for a real-time feedback system.

## References

- [1] Ozbolat, I. 3D Bioprinting Fundamentals, Principles and Applications. 1 edition, 2016.
- [2] Shafiee, A. and Atala, A. Printing Technologies for Medical Applications. Trends in Molecular Medicine 22 (3), 254-265, 2016

## Acknowledgements

The project was supported by RegenHu and HuCE-optoLab. Both entities are gratefully acknowledged.

# Optomechanical Simulations of Laser Refractive Surgeries

Simone Poncioni



Supervisors: Dr. Miguel Ángel Ariza Gracia, Prof. Dr. Philippe Büchler  
 Institution: University of Bern, ARTORG Center for Biomedical Engineering Research  
 Examiners: Prof. Dr. Philippe Büchler, Dr. med. Theo G. Seiler

## Introduction

Refractive errors are one of the leading causes of visual impairment around the world and the second leading cause of blindness [1]. Over the last two decades, femtosecond laser surgery has become an increasingly popular technique to correct myopia, hyperopia, and astigmatism. This surgical technique reshapes the corneal surface to enhance patient's visual acuity. The current surgical techniques consist of either photoablation of anterior surface of the cornea –such as photorefractive keratotomy (PRK)– or intrastromal ablation, as in small incision lenticule extraction (SMILE). Despite the increasing experience and technological innovation, 15% of operations still result in an under estimation of the correction. However, the laser ablation profile is determined based on experimental nomograms, which do not explicitly account for the mechanical deformation of the cornea. By combining finite element method (FEM) to simulate SMILE surgeries and optical ray-tracing, we aim at characterising the optical impact of the biomechanical weakening of the cornea associated with this refractive intervention.

## Materials and Methods

A numerical framework was developed to perform optomechanical simulations of laser refractive surgeries based on patient-specific clinical data. The biomechanical behaviour of the tissue was modelled using a fibre-reinforced and nonlinear material, whose parameters were identified from experimental data. A custom ablation profile was reconstructed by computing the wavefront aberration error (WA) using optical ray-tracing. The patient's corneal mesh is subsequently used to simulate post-surgical mechanical stability using a FE software (Abaqus, Dassault Systèmes). Ultimately, the patient's post-surgical WA was evaluated to assess the success of the virtual surgery [2].

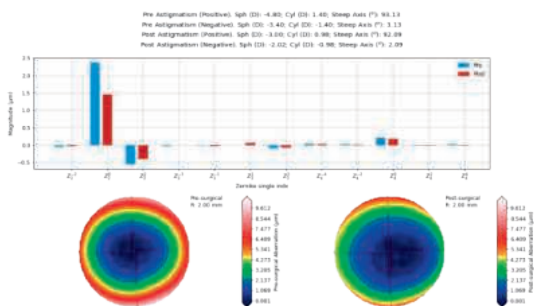


Fig. 1 Patient-specific pre- and post-surgical wavefront aberrations

## Results

A study was conducted on a virtual cohort of 60 patients undergoing SMILE surgery. Initial investigations show an overall improvement in visual acuity (Fig 1). This improvement was directly proportional to the thickness of the lenticule. However, if the pre-surgical spherical equivalent (SE) was greater than 2.5D, the postoperative visual acuity was not satisfactory, with values of spherical equivalent above 1D (Fig. 2).

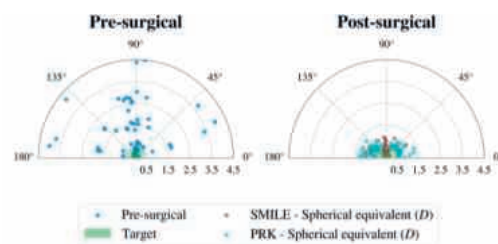


Fig. 2 Pre- and post-surgical visual acuity (SE). The target region (in green) corresponds to a successful intervention (SE < 0.5 D).

## Discussion

Our model shows how the post-surgical mechanical behaviour of the cornea is affected by the removal of the lenticule. Larger corrections (SE >2.5D) appear to be of more significant mechanical influence in the correction due to the increased tissue removal. Therefore, it is speculated that the mechanical properties of the removed material lead to an overall reduction in corneal stiffness, and thus to a corneal reshaping that cannot be predicted by planning the intervention solely based on the patient's anatomy. This Master's thesis is a first step towards the identification of an algorithm that predicts the best balance between postoperative visual outcome and mechanical stability based on optomechanical simulations instead of empirical nomograms. Besides, it will be possible to compare under which conditions PRK and SMILE surgeries offer the best postoperative mechanical stability. Further investigation into the identification of the material properties will allow to validate the model and thus achieve a more accurate prognosis.

## References

- [1] World Health Organization, *World report on vision*. WHO, 2019.
- [2] M. Á. Ariza-Gracia, J. Flecha-Lescún, J. F. Rodríguez Matas, and B. C. Calzada, "Personalized Corneal Biomechanics," M. H. B. T.-A. in B. and T. R. Doweidar, Ed. Academic Press, 2019, pp. 3–20.

# Development of an Implantable Wireless Sensor System

Simon Gabriel Rohrbach



Supervisors: Dr. Pascal Olivier Gaggero, Prof. Daniel Debrunner  
Institutions: Balluff AG  
Bern University of Applied Sciences, Institute for Human Centered Engineering HuCE  
Examiners: Prof. Dr. Volker M. Koch, Dr. Pascal Olivier Gaggero

## Introduction

Mastitis, lameness and fertility are the three major problems in today's dairy farming industry causing considerable monetary damage. Current solutions include surface-based temperature and activity measurements as well as in body measurements in the form of rumen boluses for health monitoring and heat detection. Rumen based temperature measurements are affected by heat-producing microorganisms and surface measurements are influenced by the environment. As a solution for these issues, a novel wireless sensor implant for long-time temperature and activity monitoring is proposed. The sensor is designed to send sensor data from within the cow's body while being powered by a single ½ AA lithium battery during five years.

## Materials and Methods

Suitable electronic components were researched and a miniaturized prototype was developed using the electronic design software EAGLE from Autodesk. Next to the main electronics, including microcontroller, power management, radio, accelerometer and temperature sensor, antennas were evaluated in a 0.9% saline phantom using return loss measurements with a Vector Network Analyzer (VNA). The working prototype was further tested in terms of power consumption and RF performance through the RF-phantom. Current measurements were done using a combination of a Picoscope and a CurrentRanger from Lowpowerlabs. Based on the measured current consumption at 40°C, the maximal battery life was determined.



Fig. 1 The developed wireless sensor attached to its ½ AA lithium battery next to the 3D-printed capsule implant.

The Effective Signal Power was calculated using RSSI and SNR values received from a Multitech conduit AP gateway. An estimation of the maximal

range was made based on measurements at multiple distances.

## Results

The measured average current consumption was between 7.3µA and 48µA depending on the configuration of the transceiver settings. With the selected lithium battery, the implant can function between 4.3 to 23 years. In the transmission measurements, a remaining link margin of 25dB at a distance of 16m was found. This leads to an estimated range of around 200m for out-body RF transmissions.

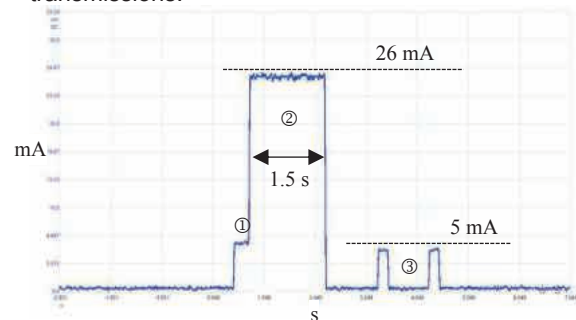


Fig. 2 Typical current consumption during a transmission cycle. The activation of the microcontroller ① is followed by the transmission frame ② and two small receive frames ③.

## Discussion

The developed prototype shows excellent low-power performance in the tests. The RF performance did show some inconsistencies, which are suspected to be caused by reflecting objects in the measurement environment. It was experimentally demonstrated that the goal of 5 year battery life is achievable. Future work shall investigate the in-vivo performance of the implant.

## References

L. C. Hicks, W. S. Hicks, R. A. Bucklin, J. K. Shearer, D. R. Bray, and P. Soto and V. Carvalho, "Comparison of Methods of Measuring Deep Body Temperatures of Dairy Cows," 2013.

## Acknowledgements

The project was supported by the innovation team at Balluff Switzerland. The availability of infrastructure such as production facilities and specialized equipments was greatly appreciated.

# Screen Calibration System for Virtual Reality Devices

Lynn Roth



Supervisors: Prof. Dr. Raphael Sznitman, Dr. Florian Stuker  
Institutions: University of Bern, ARTORG Center for Biomedical Engineering Research,  
Federal Institute of Metrology METAS  
Examiners: Prof. Dr. Raphael Sznitman, Dr. Florian Stuker

## Introduction

Glaucoma is group of eye diseases that causes progressive vision loss and can lead to total blindness [2]. Once diagnosed, glaucoma can be monitored with regular perimetry tests [1]. Standard automated perimetry consists of an analysis of the visual field of the patient by evaluating his reaction to a sequence of white stimuli projected on a screen at different locations while the brightness of the stimuli changes. Virtual reality (VR) is an emerging solution in ophthalmic technologies and, therefore, a perimetry test is implemented in a VR device to take advantage of the portability, comfort and low cost, unlike standard perimeters. However, the optical system of those VR devices is not yet fully understood, neither controlled. Therefore, we propose to validate perimetry testing with VR devices by calibrating the display. We concentrate our work on the luminance and the color to control the stimulus seen by the patient

## Materials and Methods

First, we show the influence of the temperature and the battery level on the luminance. Then, we determine the relation between the R,G,B values that are implemented in the device and the measured luminance.

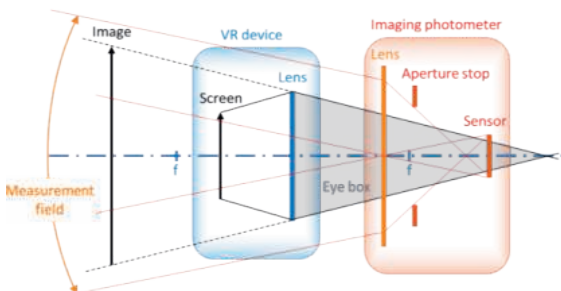


Fig. 1. Optics principle of the setup to measure the absolute luminance. The measurement field of the imaging photometer is larger than the image of the display.

We propose a measurement setup (Fig. 1) which reproduces the human eye to measure the luminance distribution on the screen. The entrance pupil of the photometer is located in the eye box of the VR device and it turns around the rotation center of its lens. Finally, a spectral analysis is performed to

define the color of the white light emitted by the screen.

## Results

We validated that the effect of temperature and battery level is negligible for a perimetry test with the VR device Oculus Quest. The relationship between the R,G,B values and the luminance is not linear. The saturation of the red and green channels changes the emitted white light. This is confirmed by the spectral analysis. The maximum luminance distribution is in the range of 78 cd/m<sup>2</sup> to 88 cd/m<sup>2</sup>. The maximum luminance depends on the screen itself but always shows a brighter spot in the center (Fig. 2).

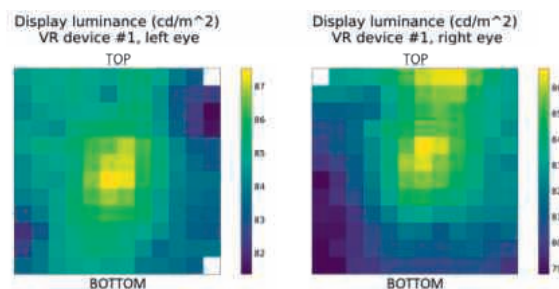


Fig. 2. Average luminance distribution measured on the left and right screen of the device.

## Discussion

The R,G,B values can be used from 90 to 255. However, the acceptable color deviation to validate a perimetry test is not yet defined. While the necessity of the color correction remains an open question, the luminance must be adjusted to obtain a stimulus with a constant brightness independent on its location. However, the current imaging photometer does not mimic perfectly the human eye. Further research has to be done on the light propagation in the system and its impact on the measurement given by the photometer.

## References

- [1] Weijland, F. Fankhauser, H. Bebie, and J. H. B. Flammer. Automated perimetry : visual field digest. Haag-Streit AG, Köniz/Bern, 5th edition
- [2] R. N. Weinreb, T. Aung, and F. A. Medeiros. The Pathophysiology and Treatment of Glaucoma: A Review. JAMA, 311(18):1901–1911, 05 2014

# Automated Quantification of Cartilage Quality for Hip Treatment Decision Support

Adrian Ruckli



Supervisors: Dr. Nicolas Gerber and Dr. Guodong Zeng  
Institution: University Bern, sitem Center for Translational Medicine and Biomedical Entrepreneurship  
Examiners: Dr. Kate Gerber and Dr. Nicolas Gerber

## Introduction

Hip cartilage quality is a major predictor of surgical outcome for the correction of femoroacetabular impingement and hip dysplasia. It can therefore be used to identify patients suitable for the minimally invasive correction and those who would benefit more from a total hip replacement. The current gold standard for assessing the cartilage quality is a visual review of 2D reformatted biochemical MR images (delayed gadolinium-enhanced MRI of cartilage, dGEMRIC) by an expert. This method is prone to inter- and intraobserver variability and requires approximately 1.5 to 2 hours assessment time for an experienced clinician which ultimately limits its use for clinical routine. A concept for automated cartilage quality analysis has been demonstrated by Schmaranzer et al., however, the method did not allow visualisation of the cartilage thickness, calculation of the weight-bearing area, and the analyse could only be performed in cooperation with an engineer. This thesis aims to develop a complete software system able to support clinicians in assessing the quality of the hip cartilage by efficiently presenting clinically relevant parameters, such as image index, volume, thickness and weight-bearing area extracted from dGEMRIC.

## Materials and Methods

A new C++ application was developed for automatic quantification of cartilage quality from dGEMRIC. The software includes novel deep learning based segmentation of the cartilage using a two-stage network architecture similar to that proposed by Schmaranzer et al. Additionally, a fully automated cartilage splitting pipeline for the central / peripheral split, femoral / acetabular split, and standardised clock face positions was implemented. For each subsection of the cartilage, the dGEMRIC index, the standard deviation, the volume, the weight-bearing area, and the thickness were calculated. Additionally, color-encoded 3D surface maps were implemented to display the cartilage dGEMRIC index, thickness, and 3D position representations. Performance of the deep learning models were evaluated using the average Dice coefficient compared to values from Schmaranzer et al.

## Results

The developed application can: load flip angle and T1 weighted images (dGEMRIC); fully automatically extract the different metrics; and display results as color-encoded 3D surface maps. The average Dice

coefficient of the segmentation was found to be  $88 \pm 3\%$ . The different quality metrics deliver results consistent to manual methods. Clinicians were able to perform a complete diagnosis within 10 minutes using a modern computer.

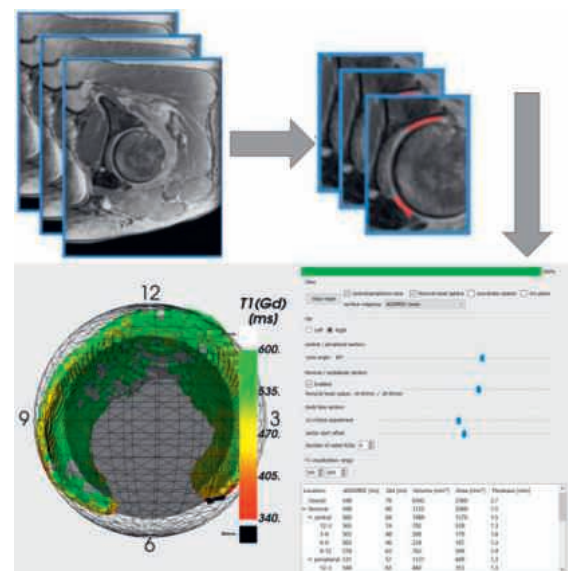


Fig. 1 Schematic illustration of the segmentation pipeline and the graphical visualization of the patient specific results. The graphical user interface provides a 3D viewer to display different surface maps, a table of the different extracted metrics, and a section for user inputs.

## Discussion

The proposed application is the first program able to provide patient-specific 3D analysis of the hip cartilage from dGEMRIC automatically. The new implementation performs 2% better on the mean Dice coefficient compared to the work of Schmaranzer et al. and allows clinicians to perform reliable analysis of a patient's hip cartilage within 10 minutes. The proposed methodology is, therefore, potentially applicable in clinical settings and could be used as a clinical decision support tool in the future.

## References

F. Schmaranzer, R. Helfenstein, G. Zeng, T. D. Lerch, E. N. Novais, J. D. Wylie, ..., G. Zheng. Automatic MRI-based Three-dimensional Models of Hip Cartilage Provide Improved Morphologic and Biochemical Analysis: Clinical Orthopaedics and Related Research, 477(5):1036-1052, May 2019

# Dense Depth Estimation in Stereo Endoscopy

Sebastian Schmid



Supervisors: Prof. Dr. Raphael Sznitman, MSc Thomas Kurmann  
Institution: University of Bern, ARTORG Center for Biomedical Engineering Research  
Examiners: Prof. Dr. Raphael Sznitman, Dr. Mathias Gallardo

## Introduction

An increasing number of minimally invasive surgeries is performed on the da Vinci surgical system, which features a binocular stereoscope [1]. The image data can be used to reconstruct a three-dimensional representation of the scene, which is a requirement for many computer-assisted surgery techniques. Stereo reconstruction algorithms already exist for other fields of research but the surgical environment poses a number of specific challenges due to its miniature scale, extreme lighting conditions and other factors [2]. To tackle this problem, the Stereo Correspondence and Reconstruction of Endoscopic Data Sub-Challenge (SCARED) was created, providing a set of stereo images and ground truth data. The aim of this work was to develop and train a deep learning model for stereo reconstruction and to evaluate it on the SCARED test dataset.

## Materials and Methods

We studied different stereo reconstruction methods and combined them into a modularized deep learning model which predicts pixel disparity from two input color images.

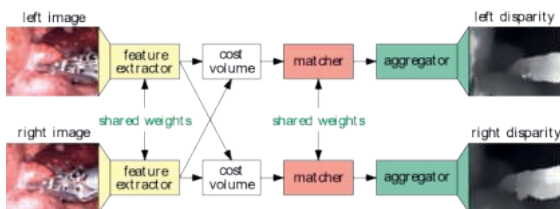


Fig. 1 Structure of deep learning model with different subunits. Processed from left to right.

Experiments were conducted on different subunits and the best performing combination was selected for the final model. To reduce the computational cost, we presented a non-uniformly strided cost volume by introducing prior knowledge about the training data. The challenge dataset was analyzed and a correction procedure was designed to improve the quality of the training data. The final model was pre-trained on the synthetic data and fine-tuned on the corrected SCARED training set using a semi-supervised loss function to account for sparse ground truth data. We evaluated the results qualitatively and using different error metrics. Finally, the model was compared to other submissions of the SCARED challenge.

## Results

On the SCARED challenge test dataset, our model achieved an average depth error of 2.66 mm, outperforming the winner of the challenge (3.04 mm). Inference times of 80 milliseconds per prediction were measured while preserving accuracy compared to other methods. We could also show that the corrected training data improves the accuracy of the final model. The qualitative inspection of the results revealed that our method creates larger errors at image boundaries and in regions with sharp changes in depth. During the analysis on the test dataset, outliers and other artefacts were found.

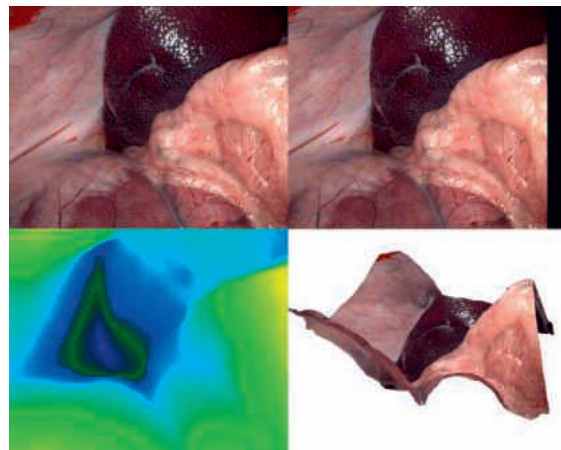


Fig. 2 Example of left/right stereo pair (top row) with estimated left disparity map (bottom left) and 3D reconstruction of the scene (bottom right).

## Discussion

We could show the introduction of prior knowledge allows for a lighter model with faster inference times while preserving accuracy. Furthermore, the improved results on the corrected dataset suggest that our correction method works.

## References

- [1] Azizian, M., Liu, M., Khalaji, I., Sorger, J., Oh, D., & Daimios, S. (2020). The da Vinci Surgical System. Elsevier Inc.
- [2] Maier-Hein, L., Moutney, P., Bartoli, A., Elhawary, H., Elson, D., Groch, A., ..., Stoyanov, D. (2013). Optical techniques for 3d surface reconstruction in computer-assisted laparoscopic surgery. Medical Image Analysis, 17(2013), 974-996.

# Development of a Patient Simulator Module for Virtual Reality Visual Field Testing

Simon Schweizer



Supervisors: Prof. Dr. Raphael Sznitman, MSc Jan Stapelfeldt  
 Institution: University of Bern, ARTORG Center for Biomedical Engineering Research  
 Examiners: Prof. Dr. Raphael Sznitman, Dr. Serife Seda Kucur Ergunay

## Introduction

Visual field (VF) testing using standard automated perimetry (SAP) is the most commonly used practice to diagnose and monitor VF defects caused primarily by glaucoma. In recent years, multiple smartphone and Virtual Reality (VR) based perimetry systems were presented to provide solutions with high portability and cost effectiveness as compared to conventional perimeters [1]. However, extensive clinical studies are necessary to validate the efficacy of new perimeters and to allow for clinical deployment [2]. The aim of this work is to extend our previously developed Oculus Quest VR perimeter with a patient response simulator to test and evaluate its performance with respect to the Open Perimetry Interface (OPI) standard.

## Materials and Methods

Our Oculus Quest VR perimetry system was extended with a patient simulator. For each location with true sensitivity threshold  $\mu$ , the probability  $P$  of seeing a stimulus of brightness  $x$  is sampled from a cumulative distribution function (CDF)  $F$  (Fig. 1). The simulator module provides two modes: A perfect mode that samples from a unit step function (Eq. 1) and a realistic mode that models response fluctuation  $\sigma$  and false positive  $fpr$  and false negative  $fnr$  responses (Eq. 2).

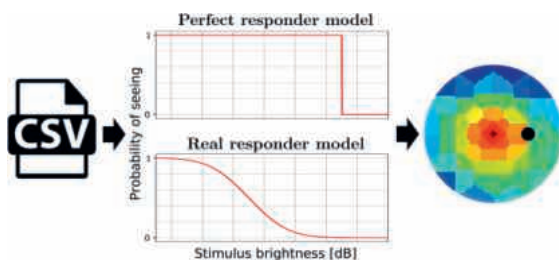


Fig. 1 Virtual measurement principle. The patient is replaced with a synthetic ground truth file and a responder model that provides answers by sampling from a CDF evaluates incoming stimuli.

$$P = \begin{cases} 0, & \text{for } \mu < x \\ 1, & \text{for } \mu \geq x \end{cases} \quad (1)$$

$$P = fpr + (1 - fpr - fnr) \cdot (1 - F(x, \mu, \sigma)) \quad (2)$$

Using the VR system and the OPI's simulated machine, both the dynamic strategy (DS) and the tendency oriented perimetry (TOP) strategy were applied to measure (I) a normal VF, (II) a VF with arcuate defect in the upper hemifield, (III) a progressing local defect and (IV) 50 real VFs. Test-retest

variability (TRV) and mean defects (MD) were compared to quantify the agreement between the VR system and the OPI's simulator.

## Results

Using the DS and the exact responder model, the MD obtained with the VR system highly correlated with the MD by the OPI ( $r = 0.99, P < 0.001$ ) (Fig. 2.a). For the realistic model, the DS correlation was slightly lower ( $r = 0.93, P < 0.001$ ). Furthermore, the TRV was shown to be lower with the VR system's DS. Measured with the TOP strategy and the exact responder, the MD by the VR system also highly correlated with the MD by the OPI ( $r = 0.97, P < 0.001$ ) (Fig. 2.b).

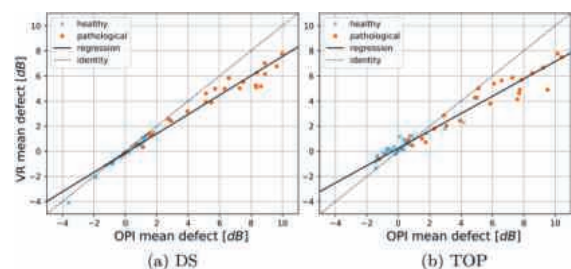


Fig. 2 MD correlation with perfect responder. (a) DS with slope  $0.77 \pm 0.05$  and intercept  $-0.14 \pm 0.16$  dB and (b) TOP with slope  $0.69 \pm 0.05$  and intercept  $0.24 \pm 0.13$  dB (95% confidence intervals).

## Discussion

The patient simulator provides the possibility to efficiently acquire unbiased retest measurements of known VFs and therefore accurately captures the true behavior of the measurement strategies. Our VR perimetry system can obtain defects highly compatible with those by the OPI standard. However, the VR perimeter tends to underestimate large defects due to its limited luminosity bandwidth.

## References

- [1] Matsumoto, Chota et al. (2016). Visual Field Testing with Head-Mounted Perimeter 'imo'. PLOS ONE. 11.e 0161974. 10.1371/journal.pone.0161974.
- [2] Racette et al. (2016). Visual Field Digest, 6th edition 2016.

## Acknowledgements

I would like to thank Prof. Dr. Raphael Sznitman and Dr. Serife Kucur Ergunay for their supervision and expert advise. I also thank Jan Stapelfeldt for his excellent work with the VR Perimeter that made this thesis possible.

# Reverse-Engineering the Connectome from iEEG to Reveal Synaptic Homeostasis in Sleep

Jan Segessenmann



Supervisors: Prof. Dr. Jörn Justiz, MSc Benjamin Ellenberger  
Institutions: Bern University of Applied Sciences, Institute for Human Centered Engineering (HuCE)  
University of Bern, Department of Physiology  
Examiners: Prof. Dr. Walter Senn, Prof. Dr. Jörn Justiz

## Introduction

As a hypothesis about the core function of sleep, the synaptic homeostasis hypothesis (SHY) states that during sleep, the overall synaptic strength is down-scaled to ensure energetic stability despite the up-scaling of synaptic strength associated with learning during waking hours [1]. The aim of this work is to fit a biologically plausible neural network to iEEG recordings to get a connectivity matrix that describes the causal relations between iEEG trajectories (see Fig. 1).

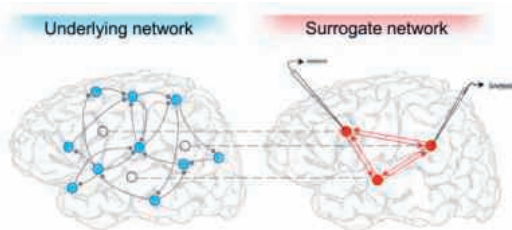


Fig. 1 Illustration of the approach. The underlying network (blue) consists of a network of biological neurons. The activity of neuron populations give rise to local field potentials (LFPs) that can be measured by iEEG. We interpret these LFPs as nodes in a surrogate network (red) that reflects features of the underlying network.

It was assumed that the resulting surrogate connectivity carries some information about the underlying biological connectivity and that it is thus possible to deduce net synaptic strength from this. We addressed the questions whether this approach is feasible and whether it is possible to confirm SHY with this approach.

## Materials and Methods

Four periods of sleep were detected and extracted from long-term iEEG recordings by studying the slow wave activity (SWA), as measured by the slow wave band power density (0.5-4 Hz). For each period of sleep, three short segments of data (with a duration of 6 minutes each) were extracted from three subsequent NREM sleep periods.

To design an appropriate model, the statistical relations between iEEG channels were studied. A semi-recurrent neural network (SRNN) was introduced, which consists of visible and hidden nodes and its states are a convex combination of current iEEG voltages and recurrent states. To study the behavior of the SRNN, a simple single-layer perceptron (SLP) was used in comparison.

For each sleep period and each subsequent short segment, both model designs were newly initialized

and fitted to the data. The resulting connectivity matrices were studied and their mean connectivities were compared.

## Results

The median correlation between predictions and targets (iEEG recordings) was 0.94 over all trained models. Using hidden nodes did not lead to a higher prediction accuracy, but instead, lead to a higher proportion of arbitrary connections. A decrease in mean connectivity from first to last segment could nevertheless be observed in the SLP for all four sleep periods. However, subsequent experiments imply that the decrease is not continuous during the night, but that it correlates with the SWA of the recordings.

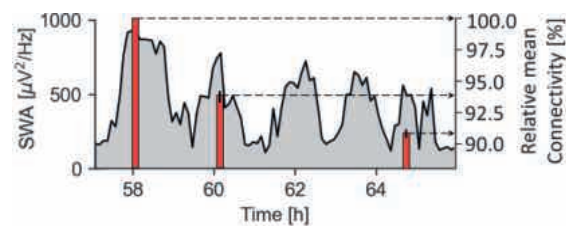


Fig. 2 SWA during one night of sleep and mean connectivity for three segments (red). The mean connectivity is shown in proportion to the one obtained from the first segment. The error bars indicate the 95% confidence interval for six attempts with varying initial connectivity.

## Discussion

For the used models, hidden nodes were of no advantage, because predicting individual iEEG channels was found to be either straight forward or too complex. It could be shown that this approach is technically and computationally feasible. The observed correlations between features of the surrogate connectivity and features of the iEEG recordings imply dependencies that should be studied further.

It cannot be stated yet whether this approach allows to deduce features of the underlying network or not. For future work, it is suggested to simulate LFPs by a known underlying network, such that dependencies between surrogate network and underlying network can be studied more directly.

## References

- [1] Tononi G. and Cirelli C., Sleep and synaptic homeostasis: A hypothesis, Brain Research Bulletin 62(2): 143-193, 2003.

# A Novel Training and Testing Simulator for PTCA Balloon Catheters

Luc Siegenthaler

Supervisors: Dr. Adrian Zurbuchen, Cornelia Amstutz  
Institution: sitem Center for Translational Medicine and Biomedical Entrepreneurship  
Examiners: PD Dr. med. Dr. phil. Andreas Haeblerlin, Dr. Adrian Zurbuchen



## Introduction

Percutaneous Transluminal Coronary Angioplasty (PTCA) balloon catheters are used to open blocked or narrowed (stenotic) coronary arteries to improve the blood flow to the heart muscle. During a minimal-invasive procedure a balloon catheter is advanced to the stenotic region with the help of a guide wire. At the target site, the balloon is inflated to dilate the narrow cross section and improve blood flow in the coronary vessel. Balloon catheters must combine different properties such as pushability, trackability, crossability and re-wrap behavior. To investigate those properties a training simulator, which mimics in-vivo-like conditions, is necessary.

## Materials and Methods

This study aimed at developing an anatomical model with material properties that are close to real aortic vessels. Therefore, seven different silicones have been selected to determine compliance by OCT measurement. Three test tubes with wall thicknesses of 0.5 mm, 1 mm and 2 mm were made from each silicone. The compliance of the silicones was compared to real coronary arteries published by Michael J.A. Williams [1]. Patient specific CT data was segmented to obtain anatomically correct geometric. The geometries were 3D printed with PolySmooth and brushed with Elastosil Vario 15A up to a wall thickness between 1 mm and 2 mm. The silicone model was released from the 3D printed cores, by acetone. All models were assembled with flange connections and positioned with stands in a PMMA basin filled with water.

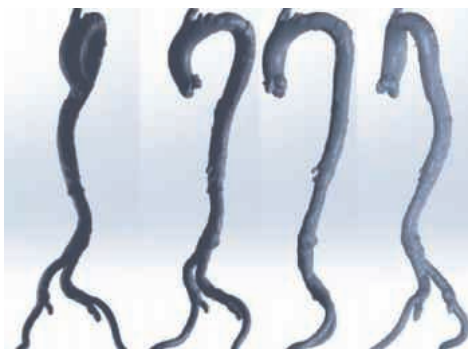


Fig. 1 Segmented aorta model from a patient specific CT scan. CAD parts were used as a positive form to create silicone models.

## Results

The result of this work is a complete and anatomically correct setup from the right iliac artery to the coronary arteries made of silicone. The coronary arteries show a physiological compliance at pressures from 90 mmHg to 120 mmHg. Furthermore, the system can be connected to an external pump to mimic pulsatile flow.



Fig. 2 Final setup of the training and testing simulator for PTCA balloon catheters. The silicone models consist of Elastosil Vario 15A.

## Discussion

Although the model has anatomically correct geometries and the coronary arteries have a physiological compliance, silicone has very poor gliding properties. A water-soap mixture significantly improved the gliding of the catheter, but this cannot yet be compared with real vessels. In order to perform scientifically significant force measurements with catheters, the gliding properties should be further improved.

## References

[1] Williams, Michael J.A. and Stewart, Assessment of the mechanical properties of coronary arteries using intravascular ultrasound: An in vivo study, 1999, doi: 10.1023/A:1006279228534.

## Acknowledgements

The support, constructive discussion and important contribution to this project of Cornelia Amstutz, Roman Bühler, Dr. Adrian Zurbuchen and PD Dr. med. Dr. phil. Andreas Haeblerlin is gratefully acknowledged.

# Computational and Experimental Investigation of the Mechanical Properties of the Human Distal Tibia

Mathieu Simon



Supervisors: MSc Denis Elia Schenk, MSc Benjamin Voumard  
Institution: University of Bern, ARTORG Center for Biomedical Engineering Research  
Examiners: Prof. Dr. Philippe Zysset, MSc Denis Elia Schenk

## Introduction

Osteogenesis imperfecta (OI) is a rare genetic disease leading to devastating bone fractures. High resolution peripheral quantitative computed tomography (HR-pQCT) provides the highest in vivo resolution for the estimation of tibial strength by finite element analysis (FEA). The aims of this study are twofold: 1) the computational assessment of fabric-elasticity relationships in OI and 2) the experimental validation of HR-pQCT-based FEA at the distal tibia..

## Materials and Methods

For the computational part, HR-pQCT scans of 120 healthy and 50 OI patients were analyzed. Fabric and stiffness tensors of cubic regions of interest (ROI) were fitted to the orthotropic Zysset-Curnier fabric-elasticity model (Fig. 1). The resulting parameters were compared between groups..

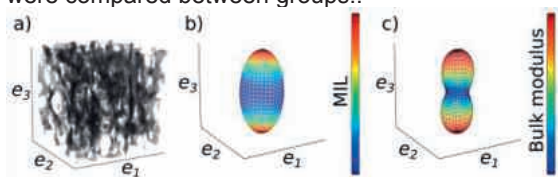


Fig. 1 a) ROI, b) fabric tensor, c) orthotropic stiffness tensor.

For the experimental part, 25 tibiae were scanned using QCT, HR-pQCT and microCT. A 30 mm section was cut out and tested in compression until failure. The HR-pQCT scans were used for homogenized finite element (hFE) analysis of a testing protocol with the same boundary conditions. Experimental and computational results for structural properties were compared. Extensive and intensive mechanical properties were then correlated with bone mineral density (BMD) and bone mineral content (BMC), respectively. Finally, a qualitative assessment of strain localization was performed with hFE results, intact and post-failure microCT scans and the resulting non-rigid registration displacement field gradient.

## Results

No significant differences in the Zysset-Curnier model parameters were found between healthy and OI patients. However, OI bone architecture presents much higher heterogeneity than healthy bone. Correlation coefficients R2 of experimental versus hFE analysis were 0.937 for stiffness and 0.945 for ultimate load. The R2 of apparent modulus and

apparent strength with BMD were 0.914 and 0.790, respectively. In turn, the R2 with BMC were 0.920 for stiffness and 0.882 for ultimate load. Image analyses showed that hFE and non-rigid registration displacement field could capture strain localization in specific cases (Fig. 2).

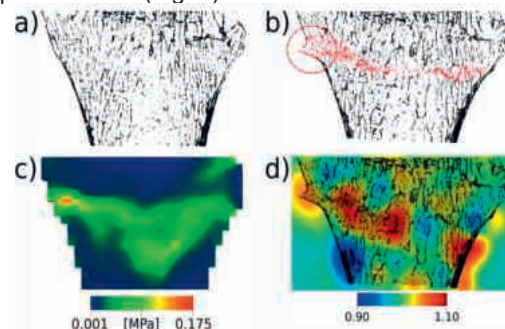


Fig. 2 Qualitative strain localisation: a) intact microCT scan, b) post-failure microCT scan, c) hFE analysis, d) non-rigid registration displacement field gradient.

## Discussion

Evaluation of trabecular architecture suggests that beyond reduced bone volume fractions, the high heterogeneity of OI bone may contribute to an increased brittleness. The strong correlations obtained between hFE and experimental stiffness and ultimate load are comparable to the ones reported in similar studies for the distal radius. The high R2 obtained for BMD with intensive properties and BMC with extensive properties are in the expected range as well. More investigations will be required for analysis of strain localisation.

## References

Panyasantisuk, J., Pahr, D. H., Gross, T., and Zysset, P. K., J Biomech Eng 137:011002, p.1-7, 2015.

## Acknowledgements

We thank Prof. M. Pretterklieber for providing the 25 tibiae and Dr. P. Varga and his team for contributing to the biomechanical tests performed at the AO foundation in Davos.

# Snap-shooting “Eureka! Brainwave”: How does Instruction Affect Task Understanding?

Shankgeeth Thadchanamoorthy

Supervisors: MSc Joaquín Á. Peñalver-Andrés, Dr. Karin A. Buetler  
Institution: University of Bern, ARTORG Center for Biomedical Engineering Research  
Examiners: Prof. Dr. Laura Marchal-Crespo, Dr. Karin A. Buetler



## Introduction

Understanding the underlying task rule is crucial for motor performance during motor training. Task instructions may be used to guide task understanding, e.g., via “Aha” experience. The “Aha” experience is usually reported when a person suddenly finds an obvious solution to a problem, but the solution approach is unclear. In contrast, analytically derived solutions are progressive with a clear solution approach. Previous studies have shown that “Aha” experienced solutions facilitate behavioral responses linked to higher cognitive functions [1]. Although several studies investigated the neural correlates of the “Aha” experience, to date, less is known about its influence on other neurocognitive and motor processes such as motor learning. This project aimed to design a novel motor task modulating the presence of “Aha” experiences during training, which could in future be used in combination with electroencephalography (EEG). The feasibility of the experimental setup and the effect of “Aha” experiences on motor performance were then investigated in a pilot study.

## Materials and Methods

Eight healthy subjects participated in a within-subject experiment. In a virtual environment, subjects sailed with a boat on the sea using a joystick (Fig. 1).

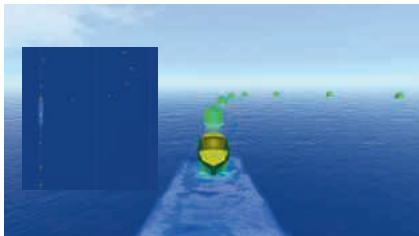


Fig. 1 First-person and top view (embedded) of the sailing game

Stimuli consisted of buoys placed in specific patterns on the sea. The patterns (stimuli) were either meaningful (letters) or random. Before the experimental trials, subjects were instructed on the sailing behavior and stimuli, and informed about the definitions of “Aha” experience and analytical problem-solving. At the beginning of each experimental trial, all buoys were green. The color of a buoy would turn yellow when the boat sailed through it. The task was to turn all buoys yellow, accelerating the boat with a button on the joystick. Once the subjects had recognized a pattern, they immediately had to press another button on the joystick that opened a questionnaire, and they were asked to report the nature of the solution finding

(“Aha” vs. analytic), and the pattern letter. We analyzed the response characteristics from the questionnaire (i.e., nature of the solution found, accuracy, response time) and motor performance variables during the task (e.g., boat acceleration after pattern recognition, and trajectory smoothness).

## Results

Questionnaire data revealed that participants recognized 68.8% of the meaningful patterns, of which 43.7% were classified as “Aha” solutions and 51.7% as analytic solutions ( $t(7) = 0.43$ ,  $p = 0.6822$ ). Further, analytic solutions were found slower ( $t(6) = -3.26$ ,  $p = 0.0173$ ), but 20% more accurately ( $t(13) = 1.70$ ,  $p = 0.1133$ ) than “Aha” solutions. Similarly, we report motor performance advantages for analytic solutions: increased boat acceleration (Fig. 2 left, +3%;  $p = 0.0025$ ) and trajectory smoothness (Fig. 2 right, +10%;  $p = 0.0975$ ) after pattern recognition.

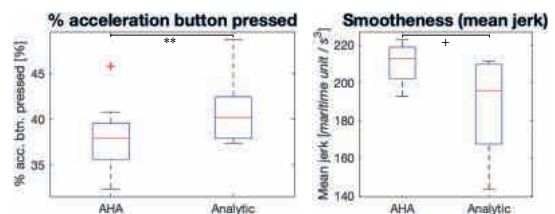


Fig. 2 Boxplots of the percentage of acceleration button pressed ( $p < 0.005$ ; \*\*) and the mean jerk ( $p < 0.1$ ; +)

## Discussion

We extend previous findings reporting faster response times for “Aha” versus analytic solutions in a novel motor task. Analytical solutions were more accurate than “Aha” solutions and associated with higher speed and smoother movements. Contrary to our hypothesis, analytically derived solutions seem beneficial for motor performance. Thus, task instructions supporting analytical thinking may be the best choice to enhance motor learning. However, future studies with larger sample sizes are required to support our conclusions. Together, we show that our motor task can be solved with “Aha” experiences and analytical problem-solving and may be suitable to investigate the neurocognitive benefits of task understanding on motor learning using EEG.

## References

[1] K. Rothmaler, R. Nigbur, and G. Ivanova, “New insights into insight: Neurophysiological correlates of the difference between the intrinsic ‘aha’ and the extrinsic ‘oh yes’ moment,” *Neuropsychologia*, vol. 95, no. December 2016, pp. 204–214, Jan. 2017.

# Particle Image Velocimetry (PIV) Measurement with in Vitro Model for Investigating the upper Urinary System

Quentin Voumard

Supervisor: Dr. Shaokai Zheng  
Institutions: University of Bern, Urogenital Engineering group,  
ARTORG Center for Biomedical Engineering Research  
Examiners: Prof. Dr. Dominik Obrist, Dr. Shaokai Zheng



## Introduction

Ureteral stents are frequently used medical devices to treat urinary obstruction, allowing the passage of urine from kidney to bladder. Kidney stones and tumors are common diseases respectively responsible for internal and external obstruction. Major complications can occur, such as reflux, stent occlusion and encrustation. These complications often lead to stent failure and urinary tract infections. According to recent studies, the fluid mechanical features of the urine flow seem to be a key aspect of the problem. This is why investigating the flow in the ureter is important. With a Particle Image Velocimetry (PIV) system, flow inside the ureter can be measured to give quantitative data. In this study, a PIV processing algorithm based on Deep Convolutional Neural Network (DCNN) is investigated, and a case study of the flow inside an in vitro ureter model is presented and briefly discussed.

## Materials and Methods

An in vitro ureter model made of silicone was used to study the flow in the upper urinary system. A PIV system was set up in the laboratory and particles were seeded in a flow loop going through the ureter model. The flow was maintained by a roller pump. A model based on DCNN was trained to provide a robust processing algorithm.



Fig. 1: One particle image of the flow inside the in vitro ureter model

The particle images were analysed with our trained neural network to provide the instantaneous velocity fields of the flow inside the ureter model.

## Results

Our DCNN model outperforms the pre-trained model in several aspects, and suffices as an accurate, efficient and robust tool for PIV analysis.

The final flow field was analyzed using 1000 particle images (500 image pairs). Every image pair provides a 2D velocity field. The vertical profile of the mean velocity field averaged over all streamwise locations is shown below, along with a theoretical velocity profile based on a Poiseuille flow.

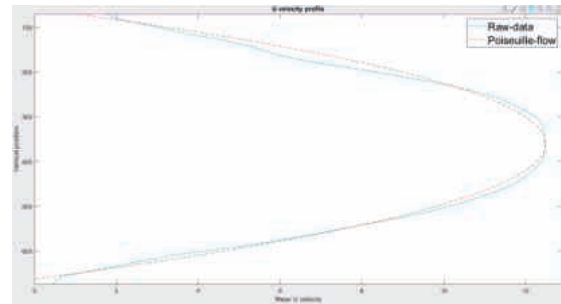


Fig. 2: Averaged velocity profile of the horizontal velocity along the vertical axis. It seems to follow a Poiseuille flow profile

## Discussion

It is possible to improve the accuracy and robustness of PIV analysis by optimizing the training strategy of the neural network. Results from our measurements show that the flow inside the ureter model follows the characteristics of a Poiseuille flow.

## References

Clavica, F., et al. (2014). Investigating the flow dynamics in the obstructed and stented ureter by means of a biomimetic artificial model. PLoS ONE, 9(2), e87433.

## Acknowledgements

Dr. Shaokai Zheng is warmly thanked for his contribution in this project. He has provided the complete PIV system and the ureter model. He has also effectively directed the whole project

# Development of a Microfluidic System for the Microvascularization of Spheroids/Organoids

Marzena Walaszczyk



Supervisors: Prof. Dr. Olivier Guenat, Dr. Soheila Zeinali  
Institution: University of Bern, ARTORG Center For Biomedical Engineering Research  
Examiners: Prof. Dr. Olivier Guenat, Dr. Soheila Zeinali

## Introduction

Animal models and conventional cell culture techniques poorly mimic human physiology. Organ-on-chips seem to be promising technology to be alternative for conventional in vitro models and refine findings from animal studies. In addition to organ-on-chip models, 3D cell constructs have been appeared such as spheroids and organoids, which are self-aggregation of cells and mini-organs presenting the key functions and structures of an organ. At a small size, they uptake nutrients via diffusion, but when they grow, diffusion is no longer possible, and a vascular network is needed to transfer the oxygen and nutrients to the central parts. Combination of these two technologies leads to spheroid/organoid-on-chips, which better mimic the in vivo environment. The goal of this combination is to perfuse 3D cell cultures with a prior grown microvasculature via vasculogenesis and angiogenesis.

## Materials and Methods

The microfluidic system is made of polydimethylsiloxane (PDMS) and comprised three layers: top, middle, and bottom. A microvasculature is grown and a spheroid is seeded in the developed chip. The microvasculature was a co-culture of endothelial cells and human fibroblasts, whereas the spheroid is made of cancerous epithelial cells. The spheroids are formed in a well plate. After 3 days of incubation, the spheroid are transferred in the chip by the help of a pipette. Then, a vascular endothelial growth factor (VEGF) gradient is generated to trigger angiogenic sprouts from the pre-existing microvasculature towards the spheroid, which will be vascularized in the future. (Fig.1)

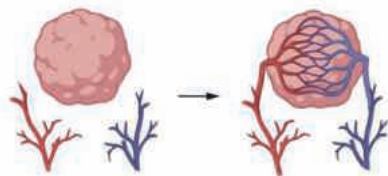


Fig. 1 Representation of the vascularization process. Sprouts are generated from a microvasculature and are attracted towards a spheroid to enhance vascularization.

## Results

This chip provided a viable environment for cells in culture. A co-culture of endothelial cells and fibroblasts is seeded into the fibrin gel and grew into

a self-assembled microvasculature network. The vessels are interconnected and form 3D lumens. With addition of the VEGF to the top of the cell culture chamber, gradient of the angiogenic growth factor is generated. This gradient conducted endothelial sprouts towards the top layer. Besides, a spheroid is successfully prepared and seeded on the top layer's gel. After 7 days of incubation, cells migrated towards spheroid from bottom layer. (Fig.2)

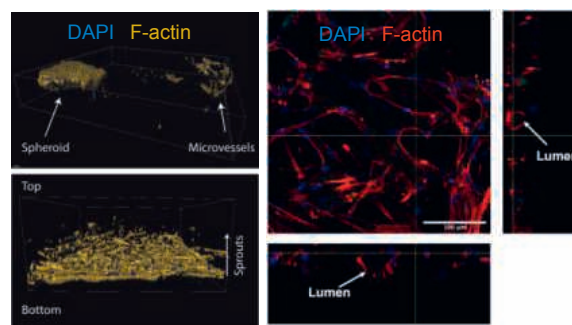


Fig. 2 3D view of the spheroid and the cells in the top layer. The microvasculature is formed and sprouts are attracted to the VEGF gradient. Orthogonal view shows 3D lumens of the microvasculature. Software: Imaris and Fiji.

## Discussion

Satisfying results are obtained, such as the microvasculature self-assembly, formation of angiogenic sprouts, and integration of a spheroid in a microvasculature-on-chip model. Further investigations will improve endothelial sprouts attraction toward the spheroid and allow to study the interaction between spheroid/organoid and microvasculature. The project aims to vascularize a spheroid to bring nutrients via vessels to the 3D constructs. Such a device will open avenue in the understanding of large tissue vascularization and can be used for drug testing in the future.

## References

Nashimoto, Y. *et al.* Integrating perfusable vascular networks with a three-dimensional tissue in a microfluidic device. *Integr. Biol.* (United Kingdom) **9**, 506–518 (2017).

## Acknowledgements

Thanks to PD Dr. phil. nat. Ren-Wang Peng for providing us cancerous epithelial cells and the equipment to create spheroids.

# Development of a Free-standing Hydrogel Layer for a Microvasculature-on-Chip through Interface Polymerization

Sandra Zwyszig



Supervisors: Prof. Dr. Olivier Guenat, MSc Dario Ferrari  
Institution: University of Bern, ARTORG Center for Biomedical Engineering Research  
Examiners: Prof. Dr. Olivier Guenat, MSc Dario Ferrari

## Introduction

Currently, in vitro microvasculature models are lacking in their ability to be adapted to tissue-specific geometries as well as in their ability to be used in perfused environments without the usage of a synthetic cell culture substrate. The first aim of this thesis is to develop a protocol for the in-chip production of a free-standing, fibrin-gel layer with a controllable thickness in the range of 75-125  $\mu\text{m}$  based on interface polymerization. The second aim is to embed human umbilical vein endothelial cells (HUVECs) in the free-standing fibrin-gel layer. The third aim is to study the ability of the HUVECs to self-assemble in a microvasculature in the fibrin layer.

## Materials and Methods

A protocol aimed at producing a fibrin-gel layer based on solid-liquid interface polymerization was developed. The interface is created within a (poly)dimethylsiloxane (PDMS) chip using a temperature gradient from 4°C to 37°C. It enabled to control the layer thickness by the polymerization time. The liquid phase consisted of 10 mg/mL fibrinogen with/without fluorescent beads and with/without embedded HUVECs with a concentration of  $10^7$  cells/mL. As a solid phase, gelatin mixed with the enzyme thrombin with a concentration of 10 U/mL, was used.

## Results

Layers of the thickness of  $61 \pm 12 \mu\text{m}$  for 25 min,  $96 \pm 9 \mu\text{m}$  for 30 min, and  $131 \pm 16 \mu\text{m}$  for 45 min polymerization time were obtained (mean  $\pm$  std. dev.,  $n=6$ ). A cross-section of the layers can be seen in

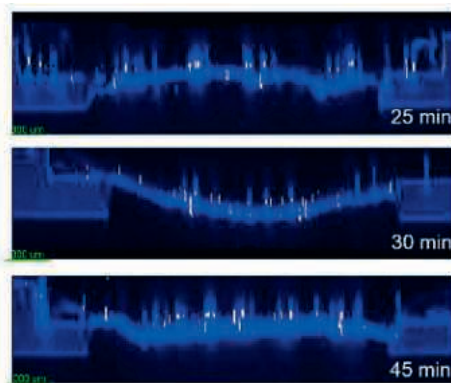


Fig. 1 Microscopy of the cross-section of the fibrin gel layers stained with Hoechst (in blue) with embedded fluorescent beads (shown in white) for polymerization times from 25 min to 45 min with a temperature gradient from 4°C to 37°C.

Fig. 1. The fibrin-gel layers with embedded HUVECs were produced with a thickness of  $99.8 \pm 7.7 \mu\text{m}$  and a polymerization time of 33 min. A maximum intensity projection and cross-section of the HUVECs embedded within the fibrin-gel layer can be seen in Fig. 2. The HUVECs did not undergo vasculogenesis, but the vasculogenic potential was shown by vascular pattern formation on the PDMS support ring (see Fig. 2). In the free-standing part of the gel layer, the cells migrated to the bottom side and formed a monolayer, which was confluent after 18 days of cultivation.

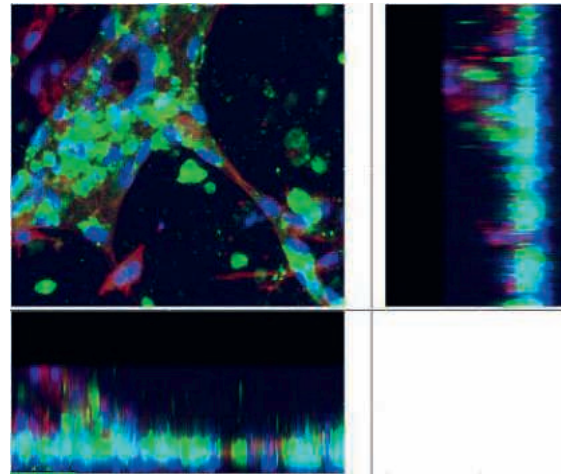


Fig. 2 HUVECs embedded in the fibrin-gel layer cultured for 5 days, located on the PDMS support ring around the free-standing fibrin-gel layer. (red: actin, green: PECAM-1, blue: cell nuclei)

## Discussion

The protocol to produce a free-standing fibrin-gel layer by interface polymerization has successfully been established with and without the embedding of HUVECs. The shapes of the layers show that the polymerization takes place at the interface between the solid and liquid phase and is driven by diffusion. The layer thickness was controlled by the incubation time, within the specified range. The HUVECs did not undergo vasculogenesis, but the vasculogenic potential was shown by vascular pattern formation on the PDMS support ring. The HUVECs in the free-standing gel migrated on the bottom side to form a confluent monolayer. This was most likely caused by mechanical strain during chip handling and by a bigger nutrient and supplement supply (e.g. VEGF) from the EGM-2 medium in the bottom channel.

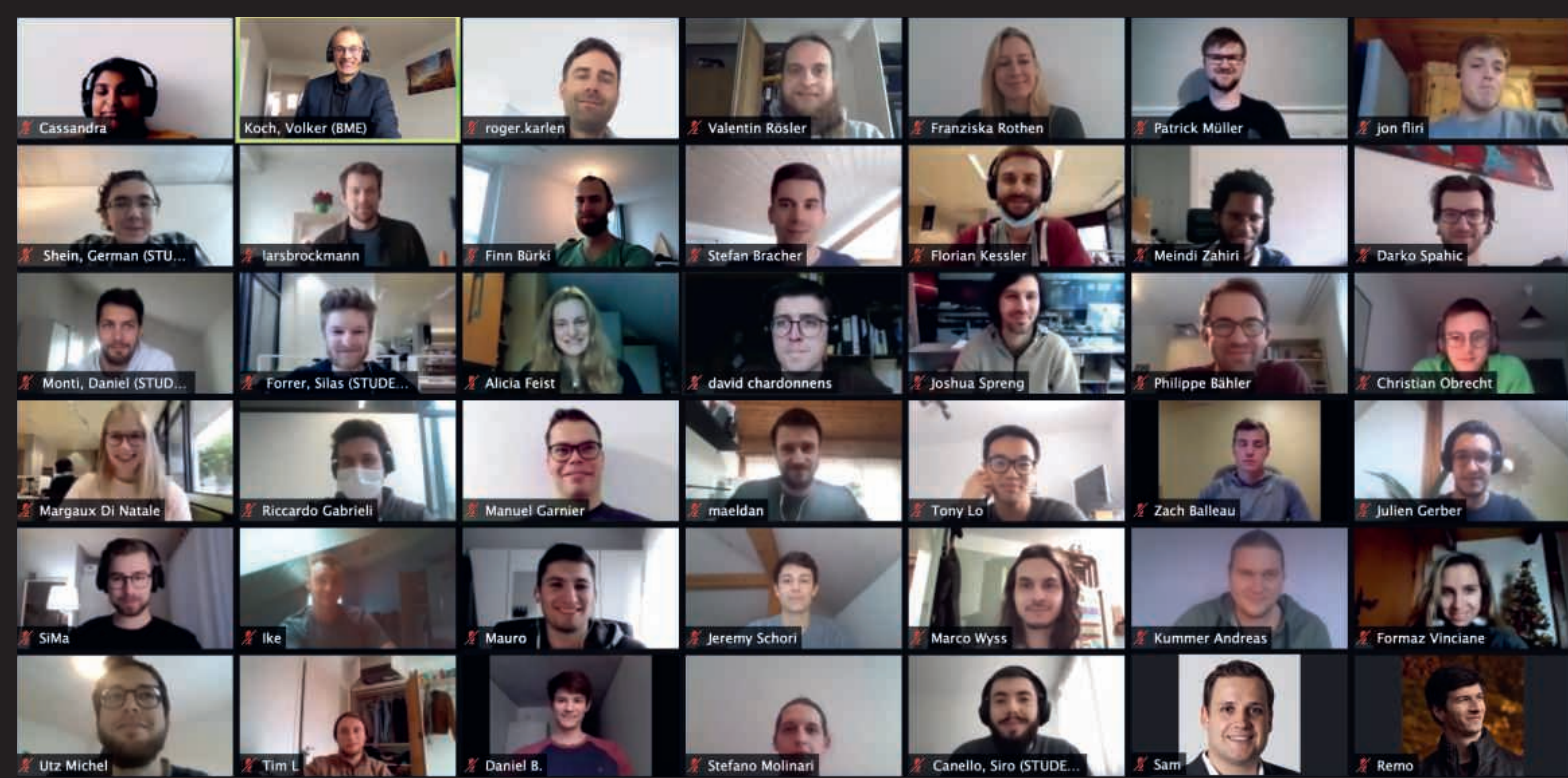
## Social Media



Follow the master's program on Instagram  
@bme\_unibe



Follow the ARTORG Center on LinkedIn  
@ [www.linkedin.com/company/artorg-center-for-biomedical-engineering-research](https://www.linkedin.com/company/artorg-center-for-biomedical-engineering-research)



## University of Bern

ARTORG Center for Biomedical Engineering Research  
Master's Program Biomedical Engineering  
Freiburgstrasse 3  
3010 Bern  
Switzerland

Phone +41 31 632 25 34/32 93  
Email [BME@artorg.unibe.ch](mailto:BME@artorg.unibe.ch)

[www.bme.master.unibe.ch](http://www.bme.master.unibe.ch)